Separation Science and Technology
Publication details, including instructions for authors and subscription information:
http://www.informaworld.com/smpp/title~content=t713708471

SEPARATION OF HYDROGEN ISOTOPES IN H_2O-H_2S SYSTEM

Boris M. Andreev[a]
[a] Department of Physical Chemistry, Mendeleev University of Chemical Engineering of Russia, Moscow, Russia

Online publication date: 30 July 2001

To cite this Article Andreev, Boris M.(2001) 'SEPARATION OF HYDROGEN ISOTOPES IN H_2O-H_2S SYSTEM', Separation Science and Technology, 36: 8, 1949 — 1989
To link to this Article: DOI: 10.1081/SS-100104764
URL: http://dx.doi.org/10.1081/SS-100104764

SEPARATION SCIENCE AND TECHNOLOGY, 36(8&9), 1949–1989 (2001)

SEPARATION OF HYDROGEN ISOTOPES IN H_2O-H_2S SYSTEM

Boris M. Andreev

Department of Physical Chemistry,
Mendeleev University of Chemical Engineering of Russia,
Miusskaya Sq. 9, Moscow 125190, Russia

ABSTRACT

The review considers thermodynamics and kinetics of isotope exchange in the H_2O-H_2S system. The temperature dependences of separation factor α are considered for all binary H-T, H-D, and D-T mixtures. The effect of equilibrium constants of homo-molecular exchange reactions involving water and hydrogen sulfide on concentration dependence of α is demonstrated. Distribution of tritium between the liquid and the gas phases has been studied as a function of the H/D ratio in each phase. The differential equations describing the steady-state interdiffusion of dissolved hydrogen sulfide and water accompanied by chemical reaction of isotope exchange have been solved. It has been shown that solution to the mass-transfer problem allows for calculation of the HTU (height of transfer unit) value in a packed separation column. The HTU dependences on the flowrate in a packed column and on the composition of liquid-phase in the H_2O-H_2S and D_2O-D_2S systems are presented. A mathematical model of isotope separation by the dual-temperature method is discussed. The model is used to analyze the basic features of the method and the effects associated with mutual solubility of phases. Optimization of the Girdler–Spevack process by varying the operation parameters in the column

are discussed. The results of testing a modified dual-temperature set-up demonstrate a high efficiency of separation of hydrogen isotopes by the proposed technique.

INTRODUCTION

Thermodynamic hydrogen isotope effect underlies the Girdler–Spevack (GS) process, which is currently the most efficient industrial method for the production of heavy water. The main advantages of this method are a high rate of isotope exchange, virtually unlimited starting material (water) supply, and a high degree of heat recuperation at the most energy-consuming stage of the process. With an increase of production of nuclear energy the problems of environment protection become a growing concern. One of these problems is the removal of radioactive hydrogen isotope (tritium) from waste waters of nuclear power stations. Solution of this problem requires utilization of methods for separation of hydrogen isotopes. Large-scale decontamination of water from tritium at nuclear power stations, at plants processing irradiated nuclear fuel, and, in the future, in tritium cycles of nuclear fusion, installations can be carried out by using the GS process. Therefore, the thermodynamic and kinetic problems of isotope exchange in the H_2O-H_2S system are of particular importance when applied to separation of binary H-T, H-D, and D-T as well as ternary H-D-T isotope mixtures.

The specific feature of the dual-temperature method has the possibility to considerably change the concentration of only one isotopic species at a virtually invariable ratio between concentrations of other isotopes. This permits applying the theory of dual-temperature method solely to separation of binary isotope mixtures. The efficiency of isotope separation and optimization of this process in production of heavy water by the GS process have been intensively studied. The vast experimental and theoretical material available on H-D exchange reactions can, therefore, be used to describe separation of tritium-containing mixtures.

THERMODYNAMICS OF ISOTOPE EXCHANGE REACTIONS

At low contents of heavy isotopes (deuterium or tritium) the following isotope exchange reactions may take place in the water–hydrogen sulfide system:

$$H_2O(liq) + HDS(gas) = HDO(liq) + H_2S(gas) \quad (1)$$

$$H_2O(liq) + HTS(gas) = HTO(liq) + H_2S(gas) \quad (2)$$

$$D_2O(liq) + DTS(gas) = DTO(liq) + D_2S(gas) \quad (3)$$

The isotope equilibrium in the above reactions and similar processes, when proceeding in the gas phase, is well-documented. The corresponding equilibrium

constants were either determined experimentally or calculated from the spectral data (for gas-phase reactions). The temperature dependences of separation factors for H-T, H-D, and D-T mixtures (or, in general cases, for mixtures of isotopes A and B) are written as follows:

$$\alpha_{gl} = a_{gl} \exp(b_{gl}/T) \quad (4)$$

$$\alpha_{g} = a_{g} \exp(b_{g}/T) \quad (5)$$

At low concentrations of the heavy isotope B the isotope exchange reactions (1–3) can be written as follows:

$$A_2O(\text{liq}) + ABS(\text{gas}) = ABO(\text{liq}) + A_2S(\text{gas}) \quad (6)$$

As seen from the data collected in Table 1, the temperature dependence of binary separation factors at low concentrations of the heavy isotope is weaker (less steep) than that at high contents of the heavy isotope. In the last case the following isotope-exchange reactions take place:

$$ABO(\text{liq}) + B_2S(\text{gas}) = B_2O(\text{liq}) + ABS(\text{gas}) \quad (7)$$

The above discrepancy can be attributed to violation of the equiprobable distribution of isotopes being separated among different types of molecules within each phase (both liquid and gaseous). The distribution is governed by the following homo-molecular exchange reactions involving water and hydrogen sulfide:

$$A_2O + B_2O = 2ABO \ (K_{ABO}) \quad (8)$$

$$A_2S + B_2S = 2ABS \ (K_{ABS}) \quad (9)$$

Assumption about a homo-molecular mechanism of exchange reactions leads to the following relation:

$$\alpha_{AB} = (K_{ABO}/K_{ABS})\alpha_{BA} \quad (10)$$

Table 1. Constants of Equation Describing Temperature Dependence of Separation Factors for Binary Isotope Mixtures in Water-hydrogen Sulfide Systems (1)

Exchanging Isotopes	High Isotope Concentrations	a_{gl}	b_{gl}	a_g	b_g
Protium-deuterium	*H*	0.855	305	1.002	237
	D	0.862	308	0.988	245
Protium-tritium	*H*	0.819	426	1.006	336
	T	0.812	433	0.962	355
Deuterium-tritium	*D*	0.951	122	0.994	103
	T	0.952	122	0.991	105

MARCEL DEKKER, INC.
270 Madison Avenue, New York, New York 10016

Since only K_{HDO} and K_{HDS} values are known from experiment, the equilibrium constants of all reactions of homo-molecular exchange of hydrogen isotopes involving water and hydrogen sulfide (K_{HDO}, K_{HTO}, K_{DTO}, K_{HDS}, K_{HTS}, and K_{DTS}) have been calculated from the data reported by Bron et al. (2). Because these data referred to molecules in the gas phase, the calculations were performed by accounting for the difference between equilibrium constants of homo-molecular exchange involving water molecules in the gas and liquid phases. The ratios of respective equilibrium constants were calculated from the separation factor values in the initial and final enrichment regions reported by Van Hook (3) by using an equation similar to Eq. (10). For any pair of isotopic molecules $K_{ABO}/K_{ABS} < 1$. Therefore the value of separation factor slightly increases with concentration of the heavy isotope. It is interesting to note that when the deviation from equiprobable distribution is maximal ($K^{\infty} = 4$), the influence of isotope composition on the value of separation factor is weaker for H-T isotopes (e.g., at 300 K $K_{HTO} = 3.716$ and $K_{HTS} = 3.771$) than for H-D exchange (at 300 K $K_{HDO} = 3.848$ and $K_{HDS} = 3.944$). The distribution of D and T isotopes is nearly equiprobable (at 300 K $K_{DTO} = 3.972$ and $K_{DTS} = 3.989$), therefore the α_{DT} and α_{TD} values are almost identical.

For reaction (1), which is used in production of heavy water, one can write the Bigeleisen equation (4):

$$\alpha_{HD,g} = 1.051 \exp(218/T) \tag{11}$$

derived by calculations from the spectroscopic data, and the relation

$$\alpha_{HD,g} = 1.010 \exp(233/T) \tag{12}$$

which together with the Kirschenbaum equation

$$1/\alpha_{HD,x} = P^{\circ}_{HDO}/P^{\circ}_{H_2O} = 1.1595 \exp(-65.43/T) \tag{13}$$

is extensively used in calculation design of industrial plants. Equations (12) and (13) give

$$\alpha_{HD,gl} = 0.871 \exp(298/T) \tag{14}$$

The relation between separation factors for binary H-T, H-D, and D-T isotope mixtures can be obtained from Eqs. (4–7):

$$\alpha_{HT} = \alpha_{HD}\alpha_{DT}\left(\frac{K_{HTO}\,K_{HDS}\,K_{DTS}}{K_{HTS}\,K_{HDO}\,K_{DTO}}\right)^{1/2} \tag{15}$$

A strong dependence of separation degree on the ratio of flow rates in the dual-temperature method allows one to reduce the problem of isotope extraction from a multicomponent mixture to separation of two isotopes at a constant concentration of other isotope species. For this, it suffices to know the dependence of the equilibrium distribution of the isotope being extracted between the liquid and the

gas phases on concentrations of other isotopes. To solve this problem, let us consider, as an example, a system where a small amount of tritium is distributed between the liquid and the gas phases at an arbitrary protium-to-deuterium ratio. At low tritium concentrations T_2O and T_2S molecules can be disregarded. By calculating protium and deuterium concentrations the contributions of HTO, DTO, HTS, and DTS molecular species can also be neglected. Therefore, the tritium distribution between phases depends on the separation factor in accordance with the following equation:

$$\alpha_T = ([\mathrm{HTO}] + [\mathrm{DTO}])/([\mathrm{HTS}] + [\mathrm{DTS}]) \tag{16}$$

By accounting for separation factors α_{HT} and α_{DT} and for the equilibrium constants of homo-molecular tritium-exchange reactions one obtains the following relation:

$$\alpha_T = \alpha_{HT} \frac{[H_2O]/[H_2S]}{1 + (K_{DTS}/K_{HTS})^{1/2} ([D_2S]/[H_2S])^{1/2}} + \alpha_{DT} \frac{[D_2O]/[D_2S]}{1 + (K_{HTS}/K_{DTS})^{1/2} ([H_2S]/[D_2S])^{1/2}} \tag{17}$$

The concentrations of molecules containing protium and deuterium in each phase can be found from known isotope compositions of water and hydrogen sulfide by using conventional methods (5)

For an equiprobable isotope distribution among molecules of various types within each phase ($K^{\infty}_{ABO} = K^{\infty}_{ABS} = 4$) Eq. (17) is simplified:

$$\alpha^{\infty}_T = \alpha_{HT} \frac{1 - x}{1 - y} = \alpha_{DT} \frac{x}{y} \tag{18}$$

where x and y are the deuterium atomic fractions in hydrogen sulfide and water, respectively. If one supposes in accordance with Eq. (15) that $\alpha_{HT} = \alpha_{HD}\,\alpha_{DT}$, this leads to the linear dependence of α^{∞}_T on deuterium concentration in the liquid phase:

$$\alpha^{\infty}_T = \alpha_{HT}(1 - x) + \alpha_{DT}\, x \tag{19}$$

For various isotopic compositions of the gas phase, one can derive the following additive relation between the reciprocal separation factors:

$$1/\alpha^{\infty}_T = [(1 - y)/\alpha_{HT}] + [y/\alpha_{DT}] \tag{20}$$

Calculations by Eqs. (17) and (19) show that at 300 K the maximum deviation of 1.2% from the linear dependence [$\Delta = (\alpha^{\infty}_T - \alpha_T)/\alpha^{\infty}_T$] is observed at $y = 0.55$.

The validity of the above theoretical relations were confirmed experimentally by Andreev et al. (6). The dependence of α_T on deuterium concentration in

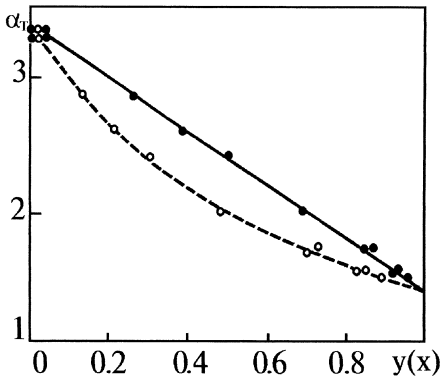

Figure 1. Dependence of separation coefficient α on content of deuterium in water (•) and hydrogen sulfide (○).

water was determined within the range from natural concentration to 0.95 atomic fraction. The experimental data (points) shown in Figure 1 are in agreement with calculated (lines) α_T versus deuterium concentration dependences both in water (solid line) and hydrogen sulfide (dotted line). A negligibly slight discrepancy between α_T values calculated by Eq. (17) and those computed by using Eqs. (18)–(20) allows one to recommend a simplified version of equations for calculations.

KINETICS OF ISOTOPE EXCHANGE AND MASS-TRANSFER EFFICIENCY

One of the main advantages of the GS process (explaining its wide industrial application for production of heavy water) is the high rate of the heterogeneous isotope exchange between water and hydrogen sulfide. The model of interphase isotope transfer, which has been proposed to describe the process, comprises the following stages:

1. diffusion in water toward liquid-gas interface;
2. isotope-exchange reaction between water and dissolved hydrogen sulfide near liquid surface;
3. reaction of interfacial isotope exchange between dissolved and gaseous hydrogen sulfide;
4. diffusion in hydrogen sulfide from the interface.

Because dissolution of hydrogen sulfide in water is a fast process, the third stage, isotope transfer, can be disregarded. In separation of hydrogen isotopes both in packed and tray-type columns, the contribution of diffusion resistance in hydro-

gen sulfide (stage 4) can also be neglected. Hence, the rate-controlling stages of the process (proceeding in the liquid phase) are the isotope-exchange reaction and reagents diffusion. The transfer of a heavy reagent (such as deuterium) from the gas to the liquid phase can be described by the following exchange reaction:

$$H_2O(\text{liq}) + HDS(\text{sol}) \underset{k_R}{\overset{k_F}{\Longleftrightarrow}} HDO(\text{liq}) + H_2S(\text{sol}), \tag{21}$$

where k_F and k_R are the rate constants of the direct and the reverse isotope-exchange reactions.

Taking into account that at low concentrations of the heavy isotope, the $[H_2O]$ and $[H_2S]$ values remain nearly constant, the second-order isotope-exchange reaction can be assumed to be of a quasi-first order whose rate is specified by the following expression:

$$-\frac{d[\text{HDS(sol)}]}{d\tau} = \frac{d[\text{HDO(liq)}]}{d\tau} = k_F^*[\text{HDO(sol)}] - k_R^*[\text{HDO(liq)}] \tag{22}$$

where $k_F^* = k_F[H_2O(\text{liq})]$ and $k_R^* = k_R[H_2S(\text{sol})]$ are the rate constants for the direct and reverse reactions of the pseudo-first order.

Isotope exchange and diffusion of reagents in the liquid phase proceed concurrently. At a steady-state profile of the isotope concentrations in a column, isotope transfer in the liquid from the interface is governed by the steady-state diffusion of reagents (dissolved gas and liquid). Under the steady-state conditions, from the material balance relations, we infer that the rates of reagent (H_2O and H_2S) diffusion and of the isotope exchange reaction are equal to

$$\begin{aligned} D_{H_2S}\frac{d^2C_y}{dl^2} &= k_F^*C_y - k_R^*C_x \\ -D_{H_2S}\frac{d^2C_x}{dl^2} &= k_F^*C_y - k_R^*C_x \end{aligned} \tag{23}$$

where D_{H_2S} and D_{H_2O} are the coefficients of molecular diffusion of hydrogen sulfide dissolved in water and of self-diffusion of water; l is the coordinate normal to the interface; $C_y = [\text{HDS(sol)}]$ and $C_x = [\text{HDO(liq)}]$ are the concentrations of respective species expressed in kmol/m^3.

Equation (23) was solved by the operator method assuming that $k_F^* >> k_R^*$ ($k_F^*/k_R^* = K = \alpha_l[H_2O(\text{liq})]/[H_2S(\text{sol})] >> 1$, because $[H_2O(\text{liq})] >> [H_2S(\text{sol})]$, and the factor of isotope separation between the liquid and the dissolved gas, $\alpha_l > 1$. The following boundary conditions were used (7):

$$\begin{aligned} \text{at } l = 0 \qquad & C_y = C_{y0}, \qquad dC_y/dl = C'_{y0} \\ & C_x = C_{x0}, \qquad dC_x/dl = C'_{x0} \end{aligned}$$

Equation (23) is valid for a diffusion boundary layer, in which the process of molecular mass transfer dominates over the turbulent transfer. The solution of these equations gives the following expression for the chemical component of the mass-transfer coefficient:

$$\beta_c = (k_F^* D_{H_2S})^{1/2} [H_2S(sol)] \tag{24}$$

As it follows from this equation, the mass-transfer coefficient β_c increases unlimitedly as the rate of isotope exchange rises. It implies that the rate of mass-transfer also increases infinitely. The gradient of isotope concentration C_{y0} depends on both the kinetics of isotope exchange reaction and the driving force at the interface, which gradually decreases with the reaction rate. Taking into account this reduction of the driving force, we obtain the resistance-additivity equation, which in the case under consideration is written as follows:

$$1/K_{0y} = 1/\beta_y + 1/\alpha\beta_x + 1/\alpha_y\beta_c \tag{25}$$

or

$$1/K_{0x} = 1/\beta_x + 1/\alpha\beta_y + \alpha_l/\beta_c, \tag{26}$$

where α_y is the separation factor corresponding to equilibrium between gaseous hydrogen sulfide and its aqueous solution, $\alpha_l = \alpha/\alpha_y$; β_x and β_y are the mass-transfer coefficients in the liquid and gas phases, respectively; K_{0x} and K_{0y} are the mass-transfer coefficients referred to the driving force in the liquid and the gas phases, respectively.

The isotope exchange between dissolved hydrogen sulfide and water may proceed via two mechanisms (7):

Mechanism I

$$H_2O + HDS(sol) \underset{k_{-1}}{\overset{k_1}{\Longleftrightarrow}} H_2DO^+ + HS^- \underset{k_2}{\overset{k_{-2}}{\Longleftrightarrow}} HDO + H_2S(sol) \tag{27}$$

The rate constants for dissociation of HDS and H_2S molecules are designated by k_1 and k_2, and the rate constants for the reverse reactions are denoted by k_{-1} and k_{-2}. The rate constants for ionic reactions are virtually independent of the isotope composition. From the equality of the rates of HDO formation and HDS consumption, which are expressed by the following equations:

$$\frac{d[HDO(liq)]}{d\tau} = k_{-2}[H_2DO^+][HS^-] - k_2[HDO(liq)][H_2S(sol)] \tag{28}$$

and

$$-\frac{d[HDS(sol)]}{d\tau} = k_1[HDS(sol)][H_2O(liq)] - k_{-1}[H_2DO^+][HS^-] \tag{29}$$

Marcel Dekker, Inc.
270 Madison Avenue, New York, New York 10016

allowing for the equality $k_{-1} = k_{-2}$, we infer that

$$\frac{d[\mathrm{HDO(liq)}]}{d\tau} = \frac{1}{2}k_1[\mathrm{H_2O(liq)}][\mathrm{HDS(sol)}] - \frac{1}{2}k_2[\mathrm{H_2S(sol)}][\mathrm{HDO(liq)}] \tag{30}$$

A comparison of this equation with Eq. (22) leads to the following relations:

$$k_F^* = 0.5\, k_1\, [\mathrm{H_2O(liq)}]$$

and

$$\beta_c = (0.5\, D_{\mathrm{H_2S}}\, k_1\, [\mathrm{H_2O(liq)}])^{1/2}\, [\mathrm{H_2S(sol)}] \tag{31}$$

Mechanism II

$$\mathrm{HDS(sol)} + \mathrm{OH^-} \underset{k_{-3}}{\overset{k_3}{\Longleftrightarrow}} \mathrm{HDO} + \mathrm{HS^-}, \tag{32}$$

$$\mathrm{HS^-} + \mathrm{H_2O} \underset{k_4}{\overset{k_{-4}}{\Longleftrightarrow}} \mathrm{H_2S(sol)} + \mathrm{OH^-}, \tag{33}$$

The rate constants for these reactions are nearly identical, and [HDS(sol) $\ll$ H_2S(sol), therefore the first reaction is the slowest one. Hence, one can write

$$\frac{d[\mathrm{HDO(liq)}]}{d\tau} = k_3[\mathrm{OH^-}][\mathrm{HDS(sol)}] - k_{-3}[\mathrm{HS^-}][\mathrm{HDO(liq)}] \tag{34}$$

By comparing this equation with Eq. (22), one obtains:

$$k_F^* = k_3\, [\mathrm{OH^-}]. \tag{35}$$

By expressing [OH^-] concentration through the equilibrium constant k_4 of reaction (33) and taking into account that equilibrium constants of reactions (32) and (33) are interrelated with each other as follows $K_3/K_4 = \alpha_l$, one can rewrite Eq. (34) in the following form:

$$k_F^* = k_3\, \alpha_l [\mathrm{H_2O(liq)}][\mathrm{HS^-}]/[\mathrm{H_2S(sol)}]$$

and

$$\beta_c = (D_{\mathrm{H_2S}}\alpha_l k_{-3}\, [\mathrm{H_2O(liq)}][\mathrm{HS^-}][\mathrm{H_2S(sol)}])^{1/2} \tag{36}$$

The efficiency of mass-exchange can be calculated from the above equations. Let us illustrate this by calculations of the chemical components β_c^I and β_c^{II} related to isotope exchange reactions of the first and second order, respectively, at $T = 303$ K and $P = 0.1$ MPa. Under these conditions, the rate constants for hydration of hydrogen sulfide and proton transfer equal $k_1[\mathrm{H_2O}] = 4.3 \cdot 10^3\ \mathrm{s^{-1}}$ and

MARCEL DEKKER, INC.
270 Madison Avenue, New York, New York 10016

$k_3 = k_4 = 5 \cdot 10^{10}$ m^3/(kmol·s), and $D_{H_2S} = 1.6 \cdot 10^{-9}$ m^2/s. The concentration $[H_2S(sol)] = [H_2O]P/H_H$ and $[HS^-] = (k_{dis}[H_2S])^{1/2}$ (the rate constant for hydrogen sulfide dissociation $k_{dis} = 10^{-7}$) can be found from the Henry's law constant for solution of hydrogen sulfide in water ($H_H = 55.2$ MPa).

The calculation results are as follows: at atmospheric pressure $\beta_c^I = 0.66$ kmol/(m^2 h) and $\beta_c^{II} = 0.047$ kmol/(m^2 h) ($\beta_c^I/\beta_c^{II} = 14$). With an increase of pressure the contribution of the exchange reaction by Mechanism II must decrease, as according to Eqs. (31) and (36), the ratio $\beta_c^I/\beta_c^{II} \sim (P)^{1/4}$. Hence, at a pressure of 2.2 MPa, which is the maximum admissible in the H_2O-H_2S system at 303 K, $\beta_c^I/\beta_c^{II} = 30$.

Thus, the isotope exchange reaction proceeds predominantly by the first mechanism. According to Eq. (31), the rate of the isotope exchange reaction rises proportionally to the hydrogen sulfide pressure. As the pressure increases, the contribution of the chemical component to the total resistance to mass transfer reduces, and at pressures above 2 Mpa, this contribution becomes apparently insignificant and the diffusion resistance dominates.

The influence of temperature on β_c^I depends on the activation energy of the hydrogen sulfide hydration reaction, which is about 25 kJ/kmol. Equation (31) shows that the temperature dependence of the diffusion coefficient of hydrogen sulfide and its solubility in water must also be taken into consideration. Although both the diffusion coefficient and the rate constant for hydrogen sulfide hydration increase with temperature, the mass-exchange efficiency only slightly depends on temperature because of substantial reduction of H_2S solubility.

The contribution of the chemical component can be reduced to zero not only by increasing the pressure but also by introducing into water some soluble compounds (salts) whose interaction with hydrogen sulfide increases concentration of OH^- and HS^- ions in the liquid phase. Thus, when salts of an acid weaker than hydrogen sulfide are added, the rate of hydrolysis of this acid, anions will be higher than that of HS^- ions. This will increase the concentration of OH^- ions. The contribution of Mechanism II to the total rate of exchange becomes dominant due to the increase of concentrations of OH^- and HS^- ions. Figure 2 shows experimental (7) and calculated (by using Eq. 36) HTU dependences on the HS^- ion concentration. Experiments were conducted with a spiral-prismatic packing with unit dimensions of 1.5 × 1.5 × 0.2-mm and a specific surface area a of 3880 m^2/m^3 at $T = 303$ K, $P = 0.1$ MPa, and $G/G^* = 0.9$.

Using Eq. (26), the HTU_{0x} value can be written in the form of a sum of the HTU components:

$$h_{0x} = h_x + (\alpha/\lambda)h_y + \alpha_l h_c \tag{37}$$

where $h_x = L_{sp}/(\beta_x a_c)$; $h_y = G_{sp}/(\beta_y a_c)$; $h_c = L_{sp}/(\beta_c a_c)$; L_{sp} and G_{sp} are the specific flow rates of the liquid and the gas phases in the column; a_c is the active area of the interface, and λ is the ratio of the flow rates.

MARCEL DEKKER, INC.
270 Madison Avenue, New York, New York 10016

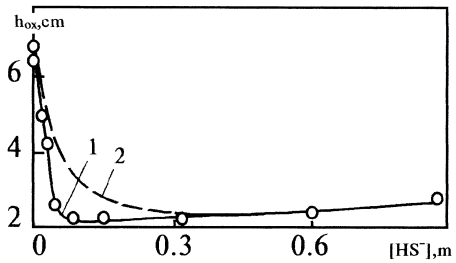

Figure 2. Experimental (1) and calculated (2) dependences of h_{ox} on concentration of HS^- ions in H-D isotope exchange.

In calculations, the h_y value was neglected and the h_x value governed by diffusion in water was calculated from the following equation:

$$Nu_x = 5 \cdot 10^3 \, d_e^{1.5} \, \mathrm{Re}_x^{0.8} \, \mathrm{Pr}_x^{0.5}$$

derived from the experimental data on rectification of H_2O-HTO mixture. As seen from Fig. 2, the calculated HTU values satisfactorily agree with the results of measurements. The horizontal section of the curve indicates the establishment of the instantaneous isotope exchange regime. The reaction rate in this regime does not influence the mass transfer process and the diffusion of water molecules becomes the rate-limiting step of the process.

The experimental data presented below are obtained for the isotope exchange in a counter-current column filled with a prismatic wire-coil packing (stainless steel) with the unit size of $1.5 \times 1.5 \times 0.2$. The results obtained are consistent with the theoretical considerations discussed above.

The HTU_{0x} dependences on the column flowrate for H-T, D-T, and H-D isotope exchange are shown in Fig. 3. The experimental dependences presented by straight lines 1–3 indicate the significance of the chemical component of HTU, whose contribution to the total resistance to mass transfer rises with the flow rate in the column. The chemical component is independent of the column hydrodynamics and for fine effective packings $a_c = \text{const}$. Therefore, the $h_{0x} = f(L_{sp})$ dependence can be plotted as a straight line whose slope at low concentrations of the heavy isotope equals $\alpha/\beta_c a_c$. Indeed, the ratio of the slopes of lines 1 and 2 obtained for H-T and H-D isotope exchange at a low deuterium concentration equals 1.34. This value is very close to the ratio of separation factors $\alpha_{HT}/\alpha_{HD} = 3.34/2.34 = 1.42$. Hence, no kinetic isotope effect is observed in the isotope exchange reactions, which allows for extension of the great body of data on the efficiency of H-D isotope exchange to separation of tritium-containing mixtures.

A weaker HTU dependence on the column flowrate observed for the D_2O and D_2S isotope exchange (see curve 3 in Fig. 3) is attributed to the fact that the

MARCEL DEKKER, INC.
270 Madison Avenue, New York, New York 10016

slope of this line must equal to $1/\beta_c \alpha a_c$ rather than to $\alpha/\beta_c a_c$. This means that at identical rates of isotope exchange the ratio of slopes of lines 2 and 3 must be close to $\alpha^2 = 2.34^2 = 5.47$. Nevertheless, the actual ratio equals 1.62, which is associated with a change in the physical properties of the D_2O-D_2S system, i.e., with reduction of the gas solubility and self-diffusion coefficient, as well as with the fact that $[D_2O(liq)] < [H_2O(liq)]$, which diminishes β_c (see Eq. 31). The identity of $h_{0x} = f(L)$ dependences for H-T and D-T isotope exchanges (see Fig. 3) in spite of the difference in the separation factors should also be attributed to the same reason.

Hence, under conditions when the chemical reaction is a rate-controlling step, the mass transfer efficiency in purifying heavy water from tritium will be lower than the efficiency of H-T separation.

The horizontal straight line 4 in Fig. 3 shows the results pertaining to the H_2O-H_2S system in the presence of a K_3PO_4 additive enhancing the isotope exchange (see above). The identity of the h_{0x} values for H-T and H-D mixtures indicates that the diffusion resistance in the liquid phase is the rate-limiting factor in this case ($\beta_{0y} > \beta_c > \beta_x$), and the mass-transfer efficiency will be virtually identical for any isotope mixture irrespective of the deuterium content.

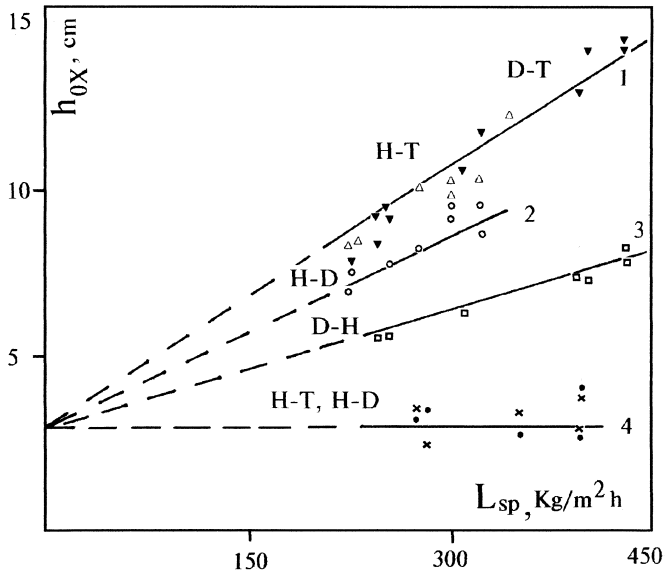

Figure 3. Influence of specific flowrate of liquid, L_{sp}, on HTU for Levin's packing in H_2O-H_2S (1, 2) and D_2O-D_2S (1, 3) systems for H-T (Δ), H-D (○), D-T (∇) and D-H (•) exchanges in absence (1–3) and in presence (4) of additive accelerating H-T (x) and H-D (•) exchanges in H_2O-H_2S system. Conditions: $T = 300$ K, $P = 0.1$ MPa.

Marcel Dekker, Inc.
270 Madison Avenue, New York, New York 10016

Table 2. Comparison of Efficiency of Different Column Packings (8)

No	Packing, Size	HTU, h_{0x}	Limiting Loading, L^*_{sp}, kg/(m^2 h)	ΔP per Transfer Unit, Pa	Intensity Factor, $F = L^*_{sp}/h_{0x}$, kg/(m^3 s)
1	Spiral-prismatic, 3.0 × 3.0 × 0.2 mm	0.03	650	120	4.2
2	ring gauze, 5 × 5 mm	0.05	1300	90	5.2
3	gauze coil, coil height = 40 mm	0.12	1900	270	3.1

Results similar to those discussed above were obtained by using separation columns with different packings (damped or preformed packing). Table 2 shows the experimental data on the efficiency of H-T and H-D isotope exchanges at $T = 300$ K and $P = 0.1$ MPa measured in different packed columns. The results collected in Table 2 show that ring gauze packing is the most efficient. It has the maximum intensity factor, which specifies the volume of separation column and the lowest pressure drop per transfer unit determining the electric energy consumption per gas circulation cycle of separation unit. When the refluxing liquid is distributed homogeneously, the mass transfer efficiency of a ring gauze packing remains almost invariable as the column diameter increases from 0.04 to 0.15 m.

STEADY-STATE MODEL OF SEPARATION COLUMNS IN DUAL TEMPERATURE SET-UP

Let us consider the steady state of a dual temperature set-up at a low concentration of the heavy isotope. The problem under consideration refers to essentially all practically important processes of hydrogen isotopes separation. Figure 4 shows a general schematic flow sheet of GS enricher with columns 1 and 2 of heights H_1 and H_2, respectively. It shows also the adopted designations of the isotope concentrations in the flows at the column ends. The steady state of the process can be described by a set of differential equations for each column as it has been reported by Rozen (5) and Bier (11):

$$L_1 \frac{dx_1}{dZ_1} = K_{oy,1}\,(y_1 - x_1/\alpha_1)a_1 S_1$$
$$G_1 \frac{dy_1}{dZ_1} = K_{oy,1}\,(y_1 - x_1/\alpha_1)a_1 S_1 \qquad (38)$$

MARCEL DEKKER, INC.
270 Madison Avenue, New York, New York 10016

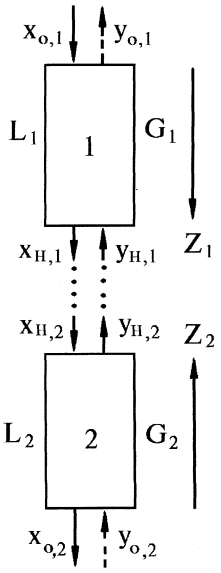

Figure 4. Schematic diagram of two jointly working columns.

$$L_2 \frac{dx_2}{dZ_2} = K_{oy,2}\,(x_2/\alpha_2 - y_2)a_2S_2$$
$$G_2 \frac{dy_2}{dZ_2} = K_{oy,2}\,(x_2/\alpha_2 - y_2)a_2S_2 \tag{39}$$

where $K_{0y,i}$ is the mass transfer coefficient; a_i is the specific area of the phases contact surface; S_i is the column cross section area; Z_i is the coordinate along column-height; α_i is the separation factor, and indices 1 and 2 denote columns 1 and 2, respectively.

The solution of the above equations will be considered for column 1 as an example. Introducing the ratio between the flow rates $\lambda_1 = G_1/L_1$ and using the expression for HTU, $h_{0y,1} = G_1/K_{0y,1}a_1S_1$ allows the set of Eq. (38) to be written as follows:

$$(\alpha_1/\lambda_1)h_{oy,1} \frac{dx_1}{dZ_1} = \alpha_1 y_1 - x_1$$
$$\alpha_1 h_{oy,1} \frac{dy_1}{dZ_1} = \alpha_1 y_1 - x_1 \tag{40}$$

MARCEL DEKKER, INC.
270 Madison Avenue, New York, New York 10016

Differentiation of the last equation gives

$$\alpha_1 h_{oy,1}\frac{d^2y_1}{dZ_1^2} = \alpha_1\frac{dy_1}{dZ_1} - \frac{dx_1}{dZ_1} \tag{41}$$

Substitution of derivatives dy_1/dZ_1 and dx_1/dZ_1 in the right-hand side of Eq. (41) through expressions given in Eq. (40) leads to the following relation:

$$\alpha_1 h_{oy,1}\frac{d^2y_1}{dZ_1^2} = (1 - \lambda_1/\alpha_1)(\alpha_1 y_1 - x_1)/h_{oy,1} \tag{42}$$

Rearrangement of the last term in the right-hand side of Eq. (42) with due regard for the second equation of set (40) leads to the following linear second-order differential equation:

$$h_{oy,1}\frac{d^2y_1}{dZ_1^2} - (1 - \lambda_1/\alpha_1)\frac{dy_1}{dZ_1} = 0 \tag{43}$$

The solution of this equation is as follows:

$$y_1 = C_1 + C_2 \exp[(1 - \lambda_1/\alpha_1)Z_1/h_{0y,1}] \tag{44}$$

To find the concentration x_1 from Eq. (44), one needs to determine derivative dy_1/dZ_1 and substitute it into the second equation of set (40)

$$x_1 = \alpha_1 C_1 + \lambda_1 C_2 \exp[(1 - \lambda_1/\alpha_1)Z_1/h_{0y,1}] \tag{45}$$

By solution of set of Eq. (39) with the following boundary conditions: $x_1 = x_{0,1}$ at $z_1 = 0$ and $x_1 = x_{\mathrm{H},1}$ at $Z_1 = H$, one obtains

$$C_1 = x_{0,1}/\alpha_1 - (x_{\mathrm{H},1} - x_{0,1})/\alpha_1 A_1 \tag{46}$$

$$C_2 = (x_{\mathrm{H},1} - x_{0,1})/\lambda_1 A_1, \tag{47}$$

where $A_1 = \exp[(1 - \lambda_1/\alpha_1)H_1/h_{0y,1}] - 1 = \exp[(1 - \lambda_1/\alpha_1)N_{y,1}] - 1$. Substitution of expressions for constants C_1 and C_2 in Eqs. (44) and (45) leads to the following relationships allowing one to calculate concentrations y_1 and x_1 at any section of column 1:

$$y_1 = \frac{x_{0,1}}{\alpha_1} - \frac{x_{H,1} - x_{0,1}}{\alpha_1 A_1} + \frac{x_{H,1} - x_{0,1}}{\lambda_1 A_1}\exp\left(\left(1 - \frac{\lambda_1}{\alpha_1}\right)\frac{Z_1}{h_{0y,1}}\right) \tag{48}$$

$$x_1 = x_{0,1} - \frac{x_{H,1} - x_{0,1}}{A_1} + \frac{x_{H,1} - x_{0,1}}{A_1}\exp\left(\left(1 - \frac{\lambda_1}{\alpha_1}\right)\frac{Z_1}{h_{0y,1}}\right). \tag{49}$$

In a similar way we can derive the dependences of concentrations y_1 and x_1 on the coordinate for column 2

$$y_2 = \frac{x_{0,2}}{\alpha_2} - \frac{x_{H,2} - x_{0,2}}{\alpha_2 A_2} + \frac{x_{H,2} - x_{0,2}}{\lambda_2 A_2} \exp\left(\left(1 - \frac{\lambda_2}{\alpha_2}\right)\frac{Z_2}{h_{0y,2}}\right) \tag{50}$$

$$x_2 = x_{0,2} - \frac{x_{H,2} - x_{0,2}}{A_2} + \frac{x_{H,2} - x_{0,2}}{A_2} \exp\left(\left(1 - \frac{\lambda_2}{\alpha_2}\right)\frac{Z_2}{h_{0y,2}}\right) \tag{51}$$

where $A_2 = \exp[(\lambda_2/\alpha_2 - 1)H_2/h_{0y,2}] - 1 = \exp[(\lambda_2/\alpha_2 - 1)\, N_{y,2}] - 1$.

Let us dwell now on the dependences of isotope enrichment on the basic parameters of a dual temperature set-up such as, separation factors (α_1 and α_2), NTU (number of transfer units) or NTP (number of theoretical plates), and the flow ratio λ_i in the columns. As both separation degrees in the cold and hot columns and their values expressed through the isotope concentrations in the liquid and the gas flows are different, the separation degrees at low concentrations of the heavy isotope are defined as follows: $K_{x,i} = x_{H,i}/x_{0,i}$ and $K_{y,i} = y_{H,i}/y_{0,i}$ The type of dependences of separation degree on the above-mentioned parameters are different for different flow sheets of the dual temperature process. At the same time, the differences among various dual temperature devices (e.g. between devices with liquid and gas feeding) may be reduced by alteration of corresponding boundary conditions upon moving from one column to another. To define these boundary conditions one needs to introduce in the general case four parameters (1). The type of the process flow sheet will be specified by two parameters defined as the ratio between concentrations in the liquid (species X) and the gas (species Y) flows at $Z_i = 0$ ($\varphi_x = x_{0,2}/x_{0,1}$ and $\varphi_y = y_{0,1}/y_{0,2}$) and two parameters depending on variations of the concentrations in each flow (X and Y) at the boundary between columns 1 and 2: ($\Psi_x = (x_{H,2} - x_{0,2})/(x_{H,1} - x_{0,1})$ and $\Psi_y = (y_{H,1} - y_{0,1})/(y_{H,2} - y_{0,2})$. The latter parameters along with appropriate values of φ_x and φ_y specify the difference in the separation degrees in columns 1 and 2

$$\begin{aligned} \Psi_x/\varphi_x &= (K_{x,2} - 1)/(K_{x,1} - 1) \\ \Psi_y/\varphi_y &= (K_{y,1} - 1)/(K_{y,2} - 1) \end{aligned} \tag{52}$$

From Eqs. (48) and (50) we find that concentrations $y_{0,1}$ and $y_{0,2}$ can be evaluated by using the following expression:

$$y_{0,i} = \frac{x_{0,i}}{\alpha_i} - \frac{x_{H,i} - x_{0,i}}{\alpha_i A_i} + \frac{x_{H,i} - x_{0,i}}{\lambda_i A_i} \tag{53}$$

Keeping in mind that $y_{0,1} = \varphi_y\, y_{0,2}$, one obtains the following equality:

$$\frac{x_{0,1}}{\alpha_1} + \frac{x_{H,1} - x_{0,1}}{\alpha_1 A_1}\left(\frac{1}{\lambda_1} - \frac{1}{\alpha_1}\right) = \varphi_y\left(\frac{x_{0,2}}{\alpha_2} + \frac{x_{H,2} - x_{0,2}}{A_2}\left(\frac{1}{\lambda_2} - \frac{1}{\alpha_2}\right)\right) \tag{54}$$

By dividing both sides of Eq. (54) by $x_{0,1}$ and expressing $x_{0,2}$ through the product $\varphi_x x_{0,1}$ and the difference between concentrations $x_{H,2} - x_{0,2}$, through the product $\Psi_x(x_{H,1} - x_{0,1})$, one obtains the following relationship:

$$\frac{K_{x,1} - 1}{A_1}\left(\frac{1}{\lambda_1} - \frac{1}{\alpha_1}\right) - \frac{K_{x,1} - 1}{A_2}\left(\frac{1}{\lambda_2} - \frac{1}{\alpha_2}\right)\varphi_y\Psi_x = \frac{\varphi_y\Psi_x}{\alpha_2} - \frac{1}{\alpha_1}. \quad (55)$$

After rearrangement of Eq. (55) we obtain the expression for enrichment of the liquid phase in column 1

$$K_{x,1} - 1 = \frac{A_1A_2(\varphi_x\varphi_y\alpha_1 - \alpha_2)}{A_1\varphi_y\Psi_x(\lambda_2 - \alpha_2)\alpha_1/\lambda_2 + A_2(\alpha_1 - \lambda_1)\alpha_2/\lambda_1} \quad (56)$$

The equation for the gas phase enrichment in column 2 can be derived in a similar way:

$$K_{y,2} - 1 = \frac{A_1A_2(\varphi_x\varphi_y\alpha_1 - \alpha_2)}{A_1(\lambda_2 - \alpha_2) + A_2\varphi_x\Psi_y(\alpha_1 - \lambda_1)} \quad (57)$$

In the operation without product withdrawal (non-withdrawal mode of operation), all four parameters equal unity, i.e., $\varphi_x = \varphi_y = \Psi_y = \Psi_x = 1$.

For a closed flow, parameters φ_x is also equal to unity and the value of parameters φ pertaining to the flow of the starting material depend on the extraction degree provided by the dual temperature set-up, i.e., $\Gamma = \Gamma_m$ (see Table 3). The equations for evaluation of Ψ_x and Ψ_y values (also given in Table 3) are derived by using the ratio $\Psi_x\Psi_y = \lambda_2/\lambda_1$, which follows from the material balance relations. The separation (extraction) degree in Table 3 and subsequent tables is

Table 3. Expressions for Calculation of Parameters φ_x, φ_y ,Ψ_y, and Ψ_x for Dual-Temperature Set-ups Operating in Different Modes by Different Process Flow Sheets

		Feeding with Liquid (X)			
		φ_x	φ_y	Ψ_x	Ψ_y
		Feeding with Gas (Y)			
Operation Regime		φ_y	φ_x	Ψ_y	Ψ_x
Without withdrawal		1	1	1	1
Second-kind withdrawal		$1 - \theta\Gamma_m^*$	1	1	1
First-kind	Concentration	$1 - \theta\Gamma_m$	1	$1/(1 - \rho)$	1
withdrawal	Depletion	1	1	$1 - \omega$	1

* $\Gamma_m = 1 - \alpha_2/\alpha_1$ is the maximum extraction degree (the extraction degree at infinitely large height of the cold and hot columns);$\Theta$is the relative yield, $\omega = W/L_2$ (W is the waste flow); $\rho = P/L_1$ (P is the product flow).

determined from the change of the isotope concentrations in the flow of starting material feeding a column. In concentrators (columns operating in an isotope concentration mode), this parameter corresponds to the separation degree K_P, which is equal to $K_{x,1}$ (when the feed-phase is X) or $K_{y,2}$ (feed is Y). In the stripping section, the separation degree K_W equals $K_{x,1}$ (when X is feed) or $K_{y,1}$ (for feeding with Y).

The column heights in Eqs. (56) and (57) are expressed through NTU values determined by the gas phase, $N_{y,1}$ and $N_{y,2}$ as in the original mass transfer Eqs. (38) and (39), the driving force is defined through the difference between isotope concentrations in the gas phase (i.e., in phase Y). In calculations through the use of transfer units determined by the liquid phase or by the theoretical plates (TP) method, the general form of Eqs. (56) and (57) remains the same. The column heights appearing in expressions for parameters A_1 and A_2 are expressed in this case through either liquid-phase NTU values (in substance Y), $N_{x,1}$ and $N_{x,2}$, or NTP, n_1 and n_2 in columns 1 and 2, respectively (see Table 4).

Unlike enrichment in conventional columns, the dual-temperature separation method exhibits a specific dependence of the separation degree on the flows ratio, which has a sharp optimum at a certain (optimal) flow-rate ratio. The optimal flow-rate ratio for all modes of operation and process flow sheets depends on the values of separation factors α_1 and α_2 and on the ratio of heights of the hot and the cold columns. The dependences of enrichment on the flow-rate ratio following from Eqs. (56) or (57) when calculated by both methods (TU and TP) are similar but are characterized by slightly different values of the optimal flow rate ratio.

In general, the analytical expression, which is used to calculate the optimal operation conditions of dual-temperature set-up providing the maximum separation degree, is based on the equality of so-called separabilities $A_1 + 1$ and $A_2 + 1$. Under these condition, one can derive from Eqs. (56) and (57) the following relation for the minimum NTU (or NTP) required to obtain a desired separation degree at the ratio of NTU (or NTP) in the hot and the cold columns κ. The κ value is expressed through either $\kappa_y = N_{y,1}/N_{y,2}$, $\kappa_x = N_{x,1}/N_{x,2}$ or $\kappa_n = n_1/n_2$ depending on the calculation method (1, 9)

$$N_1 = \kappa N_2 = a \ln[(k - u)/(1 - u)] \tag{58}$$

Table 4. Expressions for Parameters A_1 and A_2 Used in NTU and NTP Calculations

Parameter	NTU Calculations		TP Calculations
	Gas-phase	Liquid-phase	
$A_1 + 1$	$\exp((1 - \lambda_1/\alpha_1)N_{y,1})$	$\exp((\alpha_1/\lambda_1 - 1)N_{x,1})$	$(\alpha_1/\lambda_1)^{n_1}$
$A_2 + 1$	$\exp((\lambda_2/\alpha_2 - 1)N_{y,2})$	$\exp((1 - \alpha_2/\lambda_2)N_{x,2})$	$(\lambda_2/\alpha_2)^{n_2}$

Table 5. Expressions for Calculation of Optimum Ratios of Flow Rates (λ_1 and λ_2) and Parameter a in Eq. (58) with Accounting for Heights of Cold and Hot Columns (12)

Parameter	NTU Calculations		TP Calculations
	Gas-phase	Liquid-phase	
λ_1	$\dfrac{1+\kappa_y}{\kappa_y/\alpha_1+\psi_x\psi_y/\alpha_2}$	$\dfrac{\alpha_1\kappa_x\psi_x\psi_y+\alpha_2}{(1+\kappa_x)\psi_x\psi_y}$	$\sqrt[1+\kappa_n]{\alpha_1^{\kappa_n}\alpha_2/\psi_x\psi_y}$
λ_2	$\dfrac{(1+\kappa_x)\psi_x\psi_y}{\kappa_y/\alpha_1+\psi_x\psi_y/\alpha_2}$	$\dfrac{\alpha_1\kappa_x\psi_x\psi_y+\alpha_2}{1+\kappa_x}$	$\sqrt[1+\kappa_n]{\alpha_1^{\kappa_n}\alpha_2\psi_x\psi_y}$
a	$\dfrac{\alpha_1}{\alpha_1-\lambda_1}=\kappa_y\dfrac{\alpha_2}{\lambda_2-\alpha_2}$	$\dfrac{\lambda_1}{\alpha_1-\lambda_1}=\kappa_x\dfrac{\lambda_2}{\lambda_2-\alpha_2}$	$\dfrac{1}{\ln(\alpha_1/\lambda_1)}=\dfrac{\kappa_n}{\ln(\lambda_2/\alpha_2)}$

where by calculating through separation degree $K_{x,1}$

$$1-u_{x,1}=\frac{\varphi_x\varphi_y\alpha_1-\alpha_2}{\varphi_y\Psi_x(\lambda_2-\alpha_2)\alpha_1/\lambda_2+(\alpha_1-\lambda_1)\alpha_2/\lambda_1} \tag{59}$$

and through separation degree $K_{y,2}$

$$1-u_{y,2}=\frac{\varphi_x\varphi_y\alpha_1-\alpha_2}{\lambda_2-\alpha_2+\varphi_x\Psi_y(\alpha_1-\lambda_1)} \tag{60}$$

The optimal ratios of flow rates λ_1 and λ_2 when evaluated from the equality of separabilities of the cold and hot columns with due regard for the relation $\lambda_2 = \lambda_1 \Psi_x \Psi_y$ and parameter a are listed in Table 5.

At equal HTU (or HETP) values in the cold and hot columns, the maximum overall height of these columns is attained at $\kappa = 1$. Equation (58) for the minimum NTU (or NTP) and expressions for the optimum λ_1 and λ_2 values in this case are simplified. The λ_2 and λ_1 values calculated through NTP are summarized in Table 6 for all key arrangements and operation modes of dual-temperature set-ups.

Let us illustrate the dependence of separation degree $K_{x,1} = K_{x,2}$ on the flow rate ratio $\lambda_1 = \lambda_2 = \lambda$ and κ by a simple example of a dual-temperature set-up operating under non-withdrawal conditions. The dependence of separation degree on λ at $\kappa_n = 1$ for isotope exchange in the H_2O-H_2S system at $T = 303$ K and at $T = 403$ K ($\alpha_1 = 2.34$ and $\alpha_2 = 1.84$) is shown in Fig. 5 (1, 9). As the heights of the cold and the hot columns increase, the dependence of separation degree on λ becomes steeper, which necessitates a far higher accuracy to maintain the λ_0 value at a certain level. Figure 6 presents three dependences of the separation degree on κ_n at various values of λ for $\alpha_1 = 2.34$, $\alpha_2 = 1.84$, and $n_1 + n_2 = 100$ (1, 9). The curve at $\lambda = 2.075$ was computed by assuming this value to equal λ_0 (i.e., at the

Table 6. Expressions for Calculation of Optimum Flow Rate Ratios (λ_1 and λ_2) and Minimal NTP at $\kappa = 1$ (12)

Operation regime		λ_1	λ_2	$n_1 = n_2$
Without withdrawal		$\sqrt{\alpha_1\alpha_2}$	$\sqrt{\alpha_1\alpha_2}$	$\dfrac{2 \ln K_P}{\ln(\alpha_1/\alpha_2)}$
Second-kind withdrawal		$\sqrt{\alpha_1\alpha_2}$	$\sqrt{\alpha_1\alpha_2}$	$\dfrac{2 \ln((K_P - \theta)/(1 - \theta))}{\ln(\alpha_1/\alpha_2)}$
First-kind withdrawal	Concentration	$\sqrt{\alpha_1\alpha_2(1 - \rho)}$	$\sqrt{\alpha_1\alpha_2/(1 - \rho)}$	$\dfrac{2 \ln(K_P/(1 - \theta))}{\ln(\alpha_1/\alpha_2(1 - \rho))}$
	Depletion	$\sqrt{\alpha_1\alpha_2/(1 - \omega)}$	$\sqrt{\alpha_1\alpha_2(1 - \omega)}$	$\dfrac{2 \ln(K_w(1 - \theta)/(1 - \theta\Gamma_m))}{\ln(\alpha_1(1 - \omega)/\alpha_2)}$

optimal ratio of the flow rates for $\kappa_n = 1$). As might be expected, the maximum K value is attained at λ_0 and $\kappa_n = 1$. At λ_0, a deviation of κ value from 1 leads to identical reduction of enrichment degree. At another λ value, the cold and hot columns are not identical, and the maximum separation degree is observed at $\kappa_n \neq 1$.

If one of λ or κ quantities is preset, the optimal value of the other can be found from the equations listed in Table 3. It follows from these equations that in

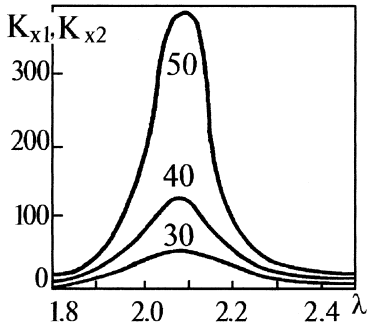

Figure 5. Dependences of $K_{x,1} = K_{x,2}$ on λ for arbitrary mode of operation and $\kappa_n = 1$ (curves correspond to different NTP values (30, 40, and 50) in one column).

Marcel Dekker, Inc.
270 Madison Avenue, New York, New York 10016

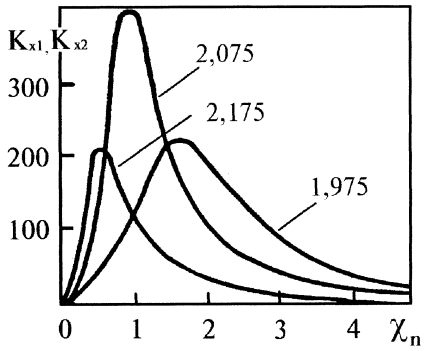

Figure 6. Dependence of $K_{x,1} = K_{x,2}$ on κ_n for arbitrary mode of operation and $n_1 + n_2 = 100$ (curves correspond to different λ values).

the non-withdrawal mode of operation and for second-kind withdrawal (i.e., at $\Psi_x = \Psi_y = 1$) an increase of κ value increases (and vice versa, reduction of κ decreases) the optimal flow-rate ratio. However, inequalities $\alpha_1 > \lambda_0 > \alpha_2$ hold at any ratio between the heights of the cold and hot columns.

Another peculiarity of the dual-temperature separation process is the dependence of isotope concentration distribution along the height of the column on the flow ratio. This dependence stems from the fact that the concentration profile depends on the mutual positions of operation lines and equilibrium curves for the cold and the hot columns on the *X-Y* diagram, which governs variations of the driving force of interfacial isotope exchange along the column height.

Figure 7 shows basic patterns of concentration variations for one of the isotopes being separated in a non-withdrawal mode of operation at its low concentration in one of the phases (12). At λ_0, the driving force of the process achieves a

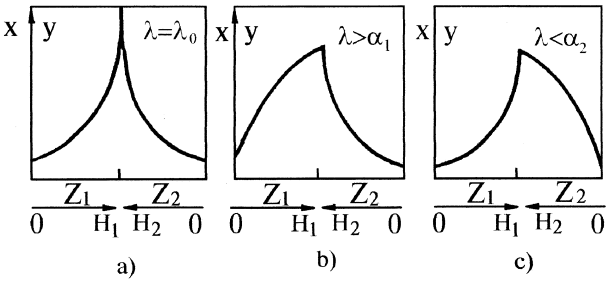

Figure 7. Basic patterns of concentration variations for one of isotopes in columns.

MARCEL DEKKER, INC.
270 Madison Avenue, New York, New York 10016

maximum and grows toward the enriched outlet zones of the cold and hot columns, i.e., in the direction of coordinate Z_1 and Z_2 (see concentration profile shown in Fig. 7a). At $\lambda > \lambda_0$, the driving force reduces in the enriched end-zone of the cold column and in the depleted end-zone of the hot column (see Fig. 7b). If $\lambda < \lambda_0$, the concentration profile in the column is similar to that shown in Fig. 7c. In particular cases when $\lambda = \alpha_1$ or $\lambda = \alpha_2$, the driving force is constant throughout the height of the cold or hot column, respectively, and the concentration dependence on column height is linear in this column.

If it is difficult to determine the isotope concentrations in the feed-flow of starting material and, hence, to calculate the concentration profile in this phase, concentrations in the circulating phase cannot be found from the material balance equations. One of the concentrations in this phase can be easily estimated by assuming the equilibrium conditions at the upper end of the cold column ($\eta_1 = x_{0.1}/\alpha_1 y_{0.1}$) and at the bottom of the hot column ($\eta_2 = \alpha_2\, y_{0.2}/x_{0.2}$). If the relative flow of withdrawal θ is known, it suffices to estimate the degree of equilibration in one of the columns as the following expression is always valid (13):

$$\eta_1\eta_2 = \alpha_2/\alpha_1\, \varphi_x\varphi_y = (1 - \Gamma_m)/(1 - \theta\Gamma_m) \tag{61}$$

The TP approach was used to derive the following equations for the equilibration degree at $n_1 = n_2$ for the second-kind withdrawal:

$$1/\eta_{\text{feed}} = 1/2 + \varphi_x\varphi_y\alpha_1/2\alpha_2, \tag{62}$$

$$\eta_{\text{waste}} = 1/2 + \alpha_2/2\alpha_1\varphi_x\varphi_y, \tag{63}$$

where for the liquid feeding $\eta_{\text{feed}} = \eta_1$ and $\eta_{\text{waste}} = \eta_2$, for the gas feeding $\eta_{\text{feed}} = \eta_2$ and $\eta_{\text{waste}} = \eta_1$.

EFFECT OF MUTUAL SOLUBILITY OF PHASES

The above-discussed theory of isotope separation by the dual-temperature method implies that the isotope-exchange process occurs between pure phases, i.e., between the liquid phase containing compound *X* and the gas phase composed of substance *Y*. However, all practically important systems including the water-hydrogen sulfide system, used in heavy water production, are characterized by fairly high solubility of one phase in the other. This results in additional circulation of gas and liquid flows, the rates of which depend on the construction and on the operation mode of the set-up. Let us consider in a general form the effects of mutual solubility of phases for a flow sheet with liquid feed and closed gas flow, which is the most interesting from the practical viewpoint. The additional flows resulting from the temperature effect of gas solubility and pressure of the saturated vapor of the liquid phase in the apparatus of this type are shown in Fig. 8.

MARCEL DEKKER, INC.
270 Madison Avenue, New York, New York 10016

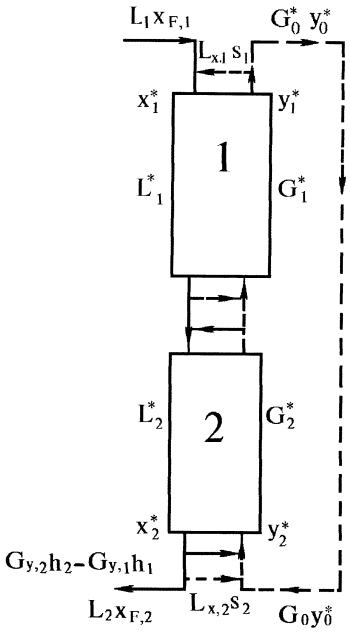

Figure 8. Scheme of flows in dual-temperature set-up with liquid feeding to cold column.

Because of the remarkable mutual solubility of phases each flow in the columns consists of two components participating in the exchange process:

$$L_i^* = L_{x,i} + L_{y,i} = L_i^*(s_{x,i} + s_{y,i}) = L_{x,i}(1 + s_i) \tag{64}$$

$$G_i^* = G_{y,i} + G_{x,i} = G_i^*(H_{y,i} + H_{x,i}) = G_{y,i}(1 + h_i) \tag{65}$$

where $L_{x,i}$ and $L_{y,i}$ are the flows of the liquid X and dissolved gas Y, respectively; L_i^* is the flow rate of the liquid with dissolved gas; $G_{y,i}$ and $G_{x,i}$ are the gas flow rates of species Y and of vapor flow of X, respectively; G_i^* is the gas-vapor flow; $s_{x,i}$, $s_{y,i}$, $H_{y,i}$, and $H_{x,i}$ are the mole fractions of X and Y in the liquid and the gas-vapor flows, respectively; s_i is the solubility of gas Y in liquid X, [mol Y/mol X], and h_i is the content of evaporated liquid X in gas Y, [mol X/mol Y].

If compounds X and Y contain different numbers of exchanging hydrogen atoms, quantities S and h must be expressed through the ratio of hydrogen gram-atoms in corresponding compounds.

The ratio of the gas and liquid flow rates can be found from the following equation:

$$\lambda_i = G_i^*/L_i^* = G_{y,i}(1 + h_i)/L_{x,i}(1 + s_i) = \lambda_i(1 + h_i)/(1 + s_i) \tag{66}$$

The feed flow F is saturated with gas, which equals $L_{x,1}s_1$, due to the contact of the feed with flow leaving column 1. Upon passing through the cold column the liquid phase heated to temperature T_2 evolves gas, which flow equals $L_{x,1}s_1 - L_{x,2}s_2$. At the outlet of the hot column, the dissolved gas is evolved from the waste liquid and then is refluxed back to the column. Its flow is equal to $L_{x,2}s_2$. It is evident that the heating of the gas flow to temperature T_2 is accompanied by formation of a flow of liquid vapor $G_{y,2}h_2 - G_{y,1}h_1$, which saturates the gas. Then this vapor is condensed upon cooling of the gas flow, which results in formation of an additional condensate flow. Some fractions of the vapor circulate along with the gas flow. For example, in dual-temperature hydrogen sulfide units operating at $T_1 = 303$ K, the steam flow saturating hydrogen sulfide in the cold column is supplied together with the gas to a circulating blower and then to the hot column.

The material balance equations for species X and Y give the following relationships for the flows in the enriched end-zone of a dual-temperature set-up operating in the enrichment (concentrating) mode with the first-kind withdrawal:

$$L_{x,2} - L_{x,1} + P = G_{x,2} - G_{x,1} = G_{y,2}\,h_2 - G_{y,1}h_1 \tag{67}$$

$$G_{y,1} - G_{y,2} = L_{y,1} - L_{y,2} = L_{x,1}s_1 - L_{x,2}s_2 \tag{68}$$

Equation (67) leads to the following expression:

$$L_{x,2}(1 - \lambda_2\,h_2) = L_{x,1}(1 - \rho - \lambda_1\,h_1) \tag{69}$$

Similarly, from Eq. (68) one obtains

$$L_{x,2}(\lambda_2 - s_2) = L_{x,1}(\lambda_1 - s_1) \tag{70}$$

Finally, we obtain

$$L_{x,2}/L_{x,1} = l = (1 - \rho - \lambda_1\,h_1)/(1 - \lambda_2\,h_2) = (\lambda_1 - s_1)/(\lambda_2 - s_2) \tag{71}$$

This expression establishes a relationship between flows in the cold (λ_1) and hot column (λ_2), which differ from each other due to the mutual solubility of phases and withdrawal of the product P. Thus, from Eq. (71) it follows that:

$$\lambda_2 = \frac{\lambda_1(1 - s_2h_1) - s_1 + s_2(1 - \rho)}{\lambda_1(h_2 - h_1) + 1 - \rho - s_1h_2} \tag{72}$$

The mutual solubility of phases must be taken into account when calculating the isotope concentration in a flow by accounting for the content of another phase in this flow with the isotope composition in question. Let us call such a concentration "effective". From material balance equation, we can obtain the following expressions for effective concentrations of the extracted isotope (14,15):

in the liquid phase $$x^* = (x + s\,y_l)/(1 + s) \tag{73}$$

in the gas phase $$y^* = (y + h\,x_g)/(1 + h) \tag{74}$$

MARCEL DEKKER, INC.
270 Madison Avenue, New York, New York 10016

Here x_g is the isotope concentration in the vapor of substance X saturating the gas phase of substance Y, and y_l is the isotope concentration in substance Y dissolved in liquid X.

The separation factor α_{gl} characterizing the principal reaction of isotope exchange, which proceeds between liquid substance X and gaseous substance Y, can be expressed through separation factor α_g describing isotope exchange in the gaseous phase and separation factor α_x associated with liquid-vapor equilibrium of substance X: $\alpha_{gl} = \alpha_g \alpha_l$.

The effect of mutual solubility on separation factor α is taken into account by introducing an effective separation factor α^* (designated frequently by β), which is defined through the ratio of effective concentrations. At low equilibrium concentrations of the heavy isotope the following relations are valid: $\alpha_x = x/x_g$ and $\alpha_y = y_l/y$. Then the effective separation factor is found from the following equation (14,15):

$$\alpha^* = \frac{\alpha + s\alpha_y}{1 + h\alpha/\alpha_x} \frac{1 + h}{1 + s} \tag{75}$$

The steady state of the processes, which is achieved under real conditions with mutual phase solubilities, can be described by the same differential Eqs. (38) and (39) if corresponding flows (L_i and G_i), concentrations (x_i and y_i), and separation factors (α_i) are substituted by their effective values (1,9). The resulting set of equations can be obviously obtained in the form of Eqs. (56) and (57) when considering all the parameters as effective quantities:

$$K^*_{x,1} - 1 = \frac{A^*_1 A^*_2(\varphi^*_x \varphi^*_y \alpha^*_1 - \alpha^*_2)}{A^*_1 \varphi^*_y \Psi^*_x(\lambda^*_2 - \alpha^*_2)\alpha^*_1/\lambda^*_2 + A^*_2(a^*_1 - \lambda^*_1)\alpha^*_2/\lambda^*_1} \tag{76}$$

$$K^*_{y,2} - 1 = \frac{A^*_1 A^*_2(\varphi^*_x \varphi^*_y \alpha^*_1 - \alpha^*_2)}{A^*_1(\lambda^*_2 - \alpha^*_2) + A^*_2 \varphi^*_x \Psi^*_y(\alpha^*_1 - \lambda^*_1)}. \tag{77}$$

Besides the above-mentioned parameters α^*_i and λ^*_i appearing also in relations (76) and (77), the effective quantities φ^*_x, φ^*_y, Ψ^*_y, Ψ^*_x, $K^*_{x,1}$, and $K^*_{y,2}$ can be expressed through effective concentrations. It should also be taken into account that under the mass-transfer conditions in counter-current units not only x_i and y_i concentrations differ from their equilibrium values but the concentration discrepancies arising due to the isotope effects in liquid evaporation or gas dissolution are also nonequilbrium. Furthermore, bearing in mind that α_x and α_y are close to unity, when calculating the effective concentrations in the columns we can assume that $x_g = x$ and $y_l = y$. Then the expressions for parameters φ^*_x, φ^*_y, Ψ^*_y, and Ψ^*_x will be read as follows (12):

$$\varphi^*_x = \frac{x^*_{0,2}}{x^*_{0,1}} = \varphi_x \frac{m + s_2/\varphi_x\varphi_y}{m + s_1} \frac{1 + s_1}{1 + s_2} \tag{78}$$

MARCEL DEKKER, INC.
270 Madison Avenue, New York, New York 10016

$$\varphi_y^* = \frac{y_{0,1}^*}{y_{0,2}^*} = \varphi_y \frac{1 + h_1 m}{1 + \varphi_x \varphi_y h_2 m} \frac{1 + h_2}{1 + h_1} \tag{79}$$

$$\Psi_x^* = \frac{x_{H,2}^* - x_{0,2}^*}{x_{H,1}^* - x_{0,1}^*} = \Psi_x \frac{1 + s_2/\lambda_2}{1 + s_1/\lambda_1} \frac{1 + s_1}{1 + s_2} \tag{80}$$

$$\Psi_y^* = \frac{y_{H,1}^* - y_{0,1}^*}{y_{H,2}^* - y_{0,2}^*} = \Psi_y \frac{1 + h_1 \lambda_1}{1 + h_2 \lambda_2} \frac{1 + h_2}{1 + h_1} \tag{81}$$

Parameters ϕ_x, ϕ_y, Ψ_y, and Ψ_x can be evaluated from Table 3, and the quantity $m = x_{0,1}/y_{0,1} = \alpha_1 h_1$ depends on the mode of set-up operation and on the θ value (for enriching set-up with withdrawal of the first- and the second kind). Although the m value can be found from either Eq. (62) or (63), for enriching columns with withdrawal of the first- and the second-kind operating at $\theta \to 0$ one can assume that $m = \alpha_1$. For purification and non-withdrawal modes of operation (at $N_1 = N_2$ and $\lambda = \lambda_0$), m can be assumed to equal λ_0.

The operation efficiency of a set-up can conveniently be characterized by a separation degree determined from the isotope concentrations in a "pure" phase, which is connected with the effective separation degree by the following equation:

$$K_{x,1}^* = x_{H,1}^*/x_{0,1}^* = (K_{x,1} + K_{y,1}\, s_1/m)/(1 + s_1/m) \tag{82}$$

The separation degree $K_{y,1}$ standing in this equation can be calculated from expression $(K_{x,1} - 1)/(K_{y,1} - 1) = \lambda_1/m$.

If $K_{x,1}$ and $K_{y,1} >> 1$, $K_{y,1} = K_{x,1}\, m/\lambda_1$ and Eq. (82) will take the following form:

$$K_{x,1}^* = K_{x,1}(1 + s_1/\lambda_1)/(1 + s_1/m) \tag{83}$$

Similarly, the following equation can be derived:

$$K_{y,2}^* = y_{H,2}^*/y_{0,2}^* = (K_{y,2} + K_{x,2}\, \varphi_x\, \varphi_y\, h_2\, m)/(1 + \varphi_y\, \varphi_x\, h_2) \tag{84}$$

and then reduces at $K_{y,2}$ and $K_{x,2} >> 1$ to

$$K_{y,2}^* = K_{y,2}(1 + h_2\, \lambda_2)/(1 + h_2\, m) \tag{85}$$

Let us dwell now on determination of the optimal ratio of flows, which in a system with mutual solubility of phases may differ from its value calculated by disregarding the additional circulation flows (i.e., by using the equations listed in Tables 5 and 6). Under these conditions the optimum corresponding to the maximum separation degree is characterized by the equality of separabilities $A_1 + 1$ and $A_2 + 1$. Their values can be evaluated by formulas listed in Table 4, in which α_i, λ_i, and N_i are substituted by their effective values. Hence, expressions for the optimal values of λ_1^* and λ_2^* can be obtained from the formulas of Table 5 upon substitution of all parameters standing in these equations by their effective values. To find parameters Ψ_x^* and Ψ_y^* one should know both λ_1 and λ_2 values corresponding to the optimal λ_1^* and λ_2^* magnitudes.

If Eqs. (76)–(85), connecting separation degree and parameters of a dual-temperature set-up, are applicable to any flow sheets and modes of operation, the values of additional circulation flows must be found for a particular set-up design. Therefore the optimal ratios of the flow rates in identical set-ups with liquid or gas feeding may differ from each other.

For example, for a dual-temperature set-up with a closed gas flow (see Fig. 8) operating in the first-kind withdrawal mode, substitution of λ_1^* and λ_2^* (with regard to Eqs. (66) and (72)) into expression $\alpha_1^*/\lambda_1^* = \lambda_2^*/\alpha_2^*$ (corresponding to the optimal condition at $n_1^* = n_2^*$ in NTP calculations) leads to the following equation of the second order in terms of the optimal flow ratio (1,9)

$$\lambda_1^2(1 - s_2h_1) + \lambda_1[(h_2 - h_1)C - s_1 + s_2(1 - \rho)] - C(1 - \rho - s_1h_2) = 0 \quad (86)$$

where $C = \alpha_1^* \alpha_2^*(1 + s_1)(1 + s_2)/(1 + h_1)(1 + h_2)$. In a system operating with the second-kind withdrawal or in a non-withdrawal mode $\rho = P/F = 0$ and Eqs. (72) and (86) are simplified.

After evaluation of the optimal flow ratios, determination of the minimum N_i value required to achieve the desired separation degree in a set-up operating with mutual solubility of the phases is substantially simplified. At $A_1 + 1 = A_2 + 1$ the following relationship is obtained from Eqs. (76) and (77) (1,9,12):

$$N_1^* = \kappa^* N_2^* = a^* \ln[(K^* - u^*)/(1 - u^*)] \quad (87)$$

where in calculations through separation degree $K_{x,1}^*$

$$1 - u_{x,1}^* = \frac{\varphi_x^*\varphi_y^*\alpha_1^* - \alpha_2^*}{\varphi_y^*\Psi_x^*(\lambda_2^* - \alpha_2^*)\alpha_1^*/\lambda_2^* + (\alpha_1^* - \lambda_1^*)\alpha_2^*/\lambda_1^*} \quad (88)$$

in calculations through separation degree $K_{y,1}^*$

$$1 - u_{y,2}^* = \frac{\varphi_x^*\varphi_y^*\alpha_1^* - \alpha_2^*}{\lambda_2^* - \alpha_2^* + \varphi_x^*\Psi_y^*(\alpha_1^* - \lambda_1^*)} \quad (89)$$

in calculations through NTU determined by the liquid- or gas-phase

$$a^* = \frac{\alpha_1^*}{\alpha_1^* - \lambda_1^*} = \kappa_y^* \frac{\alpha_2^*}{\lambda_2^* - \alpha_2^*}$$

and

$$a^* = \frac{\lambda_1^*}{\alpha_1^* - \lambda_1^*} = \kappa_x^* \frac{\lambda_2^*}{\lambda_2^* - \alpha_2^*} \quad (90)$$

in calculations through NTP

$$a^* = \frac{1}{\ln(\alpha_1^*/\lambda_1^*)} = \frac{\kappa_n^*}{\ln(\lambda_2^*/\alpha_2^*)} \quad (91)$$

Let us consider as an example the effect of mutual solubility of the phases on the optimal flow ratios and number of transfer units in the gas phase in a dual-

Table 7. Calculated Parameters of Dual-temperature Set-up ($K_W = K_P = 10$, $\theta = 0.8$) with Zero Mutual Phase Solubility (12)

Isotope Mixture	Mode of Operation	α_1	α_2	λ_1	λ_2	$N_{y,1} + N_{y,2}$
D-T	Second-kind	1.424	1.288	1.353	1.353	152.8
H-D	withdrawal	2.388	1.824	2.049	2.049	62.0
H-T		3.340	2.360	2.766	2.766	44.6
H-T	Depletion	3.340	2.360	3.249	2.492	50.6

temperature set-up separating various binary mixtures of hydrogen isotopes in the water-hydrogen sulfide system ($T_1 = 303$ K, $T_2 = 403$, $P = 2.05$ MPa, and $\theta = 0.8$) at low concentrations of heavy isotope (second-kind withdrawal for enrichment ($K_B = 10$) or depletion mode of operation). The values of separation coefficients for various binary isotope mixtures and the λ_1, λ_2 and $N_{y,1} + N_{y,2}$ values are collected in Table 7.

The values of effective separation factors α_1^* and α_2^* calculated by Eq. (75) at $s_1 = 0.03166$, $h_1 = 0.00030$, $s_2 = 0.010082$, and $h_2 = 0.15798$ (12,16) by assuming that $\alpha_y = 1$ are collected in Table 8. The optimal flow-rate ratios were calculated for a set-up with liquid feed using the procedure described above. Parameters φ_x^*, φ_y^*, Ψ_y^*, and Ψ_x^* were evaluated from Eqs. (78)–(81) and the numbers of transfer units $N_{y,1}^* = N_{y,2}^*$, from Eqs. (87), (88), and (91). The results of calculations including mutual solubility of phases are also summarized in Table 8.

A comparison of the data given in Tables 7 and 8 shows that mutual solubility of phases remarkably increases the minimum value of NTU required. Thus, in a system operating in the second-kind withdrawal mode the increase of NTU for D-T and H-T isotope mixtures achieves ~15 and 27%, respectively. In the depletion mode of operation requiring the columns of the maximal height the mutual

Table 8. Calculated Parameters of Dual-temperature Set-up ($K_W = K_P = 10$, $\theta = 0.8$) with Accounting for Mutual Phase Solubility (12)

Isotope Mixture	Mode of Operation	α_1^*	α_2^*	λ_1^*	λ_2^*	φ_x^*	φ_y^*	Ψ_x^*	Ψ_y^*	$N_{y,1} + N_{y,2}$
D-T	Second-kind withdrawal	1.409	1.237	1.347	1.292	0.930	0.960	1.005	0.988	176.2
H-D		2.289	1.636	2.048	1.808	0.834	0.891	1.011	0.875	75.6
H-T		3.248	1.987	2.791	2.267	0.776	0.831	1.012	0.804	56.9
H-T	Depletion	3.248	1.287	3.185	2.026	1.019	0.804	0.742	0.842	84.8

Marcel Dekker, Inc.
270 Madison Avenue, New York, New York 10016

phase solubility deteriorates the separation efficiency most drastically that causes the need to increase the column height by a factor of 1.5 or more.

OPTIMUM PARAMETERS AND SEPARATION FLOW SHEETS

The efficiency of the dual-temperature method of hydrogen isotope separation depends on the operation conditions, such as pressure and temperature in the cold and hot columns, which must be selected with due regard by the phase diagram of the hydrogen sulfide-water system shown in Fig. 9. The diagram shows the following phase-transitions curves:

1. hydrogen sulfide liquefaction (specifies the temperature dependence of the saturated pressure of H_2S vapor);
2. crystal hydrate formation from gaseous hydrogen sulfide and water, and
3. crystal hydrate formation from liquid hydrogen sulfide and water. The curves cross at the quadruple point ($T = 302.6$ K and $P = 2.26$ MPa) in which four phases coexist: gaseous and liquid hydrogen sulfide, water, and solid crystal hydrate with composition of $8H_2S{\cdot}46H_2O$. The

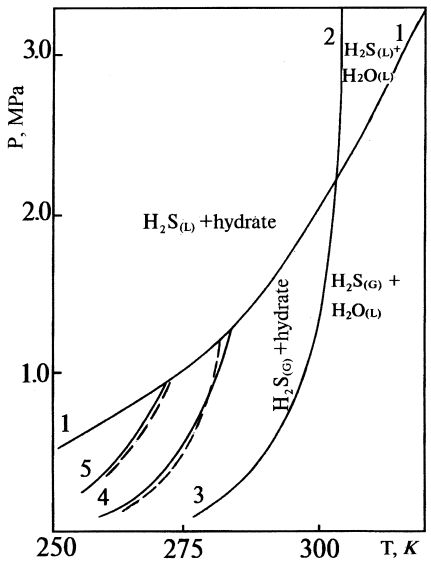

Figure 9. Phase diagram of hydrogen sulfide-water system (see text).

crystals of this hydrate resemble a snow or loose ice. Obviously, the operation conditions (pressure and temperature) in the column with counter-flows of gaseous hydrogen sulfide and water are restricted by the area under curves 1 and 2 in the phase diagram.

An increase in the temperature difference between the cold and hot columns enhances the separation efficiency (enhances both the extraction and separation degrees) in a dual-temperature set-up. However, a decrease of the temperature T_1 in the cold column necessitates reduction of pressure in accordance with curve 1 or 2 in the phase diagram, which bound the region of admissible operation parameters in a dual-temperature set-up. If the temperature and pressure are above the values corresponding to the coordinates of the quadruple point, the positive effect produced by an increase of the separation factor α_1 in the cold column upon lowering T_1 surpasses the negative effect associated with reduction of the loading capacity of the columns caused by the pressure drop (temperature T_1 and pressure P_1 vary along curve 1 in the phase diagram). When changing T_1 and P_1 below the quadruple point, one should take into account curve 2 whose slope is steeper. In this case, even a slight decrease in T_1 reduces significantly the pressure, and the loading capacity of the columns is no longer compensated by an increase of α value. Therefore, the optimum operation conditions in the cold column are controlled by the coordinates of quadruple point in the range of $T_1 = 303$–308 K and $P_1 = 2.0$–2.2 MPa.

As the temperature in the hot column increases, the energy consumption needed to heat the flows up also increases not only due to the higher difference between temperatures of the cold and hot columns, but to the larger amount of steam needed to saturate hydrogen sulfide. When the steam content in the gas flow in the hot column is high, the column cross-section must be increased. In addition, one should also keep in mind the negative effect on the separation efficiency of additional circulation flows caused by mutual phase solubility. Therefore when evaluating the hot-column temperature, one must use as the optimizing criterion an economical factor (operational costs) that accounts for the energy consumption (predominantly for heating) during the separation process and the size (capital costs) of the plant. The results of calculations reported by Burgess (17) demonstrated that at pressures being in the range of 2.0–2.2 MPa the optimal temperature in the hot-column T_2 is between 392 and 403 K.

These parameters were used as optimal in industrial plants producing heavy water by the GS method. When separating tritium-containing mixtures, the optimal temperatures and pressures in the cold column must be identical to those used in separation of H-D mixtures, because these parameters depend on the conditions of formation of crystalline hydrogen sulfide hydrate. Therefore, the determination of optimal conditions for operation of set-ups designed for separation of tritium-containing mixtures reduces to evaluation of the temperature in hot column. This temperature can be estimated by using the specific energy consumption, i.e., expenditures of energy per unit product yield.

MARCEL DEKKER, INC.
270 Madison Avenue, New York, New York 10016

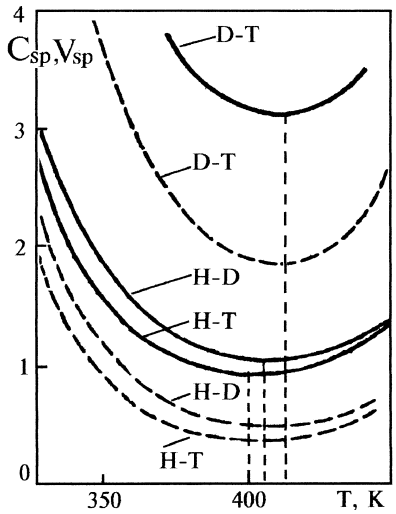

Figure 10. Dependence of C_{sp} (solid line) and V_{sp} (dotted line) on temperature of hot column.

The results of these calculations (9) are presented in Fig. 10, where the temperature dependences of the specific consumption of energy (C_{sp}) and that of the component of energy expenditure depending solely on the volume of separation column (V_{sp}) are shown. The position of minima on these curves corresponds approximately to the optimal specific energy consumption. Hence, the energy expenditures proportional to the column volume govern the optimal temperature in the hot column. As it is seen from Fig. 10, the optimal hot-column temperatures in separation of H-T and D-T mixtures are about 400 and 415 K, respectively.

It is noteworthy that at the optimal temperature of hot column the specific energy consumption C_{sp} in separation of H-T isotope mixtures is only slightly smaller than that in separation of H-D mixtures. This is attributed to the fact that the positive effect associated with an increase of extraction degree and with reduction of the number of transfer units due to the steeper temperature dependence of the separation factor α_{HT} is compensated by the negative effect produced by an increase in the flow rate ratio due to higher values of separation factors at these temperatures. This leads to an increase in the column cross-section and in the additional heat consumption for saturation of the gas flow by water steam.

The specific energy consumption in separation of deuterium-containing mixtures is almost three times as high as that in deuterium enriching. This is caused by a considerable increase in NTU (about 3-fold) and reduction of the extraction degree (approximately by a factor of two).

MARCEL DEKKER, INC.
270 Madison Avenue, New York, New York 10016

The study of phase equilibrium in the H_2S-H_2O system have revealed that the quadrupole point (see Fig. 9) can be considerably shifted after introduction of water soluble additives in the liquid phase (18). This enables one to significantly decrease the temperature in the cold column due to the reduction of pressure in conformity with curve 1 (see Fig. 9) of hydrogen sulfide liquefaction. If in lowering the pressure the temperature in the cold column is assumed to be 5° higher than the liquefaction temperature, and the hot-column temperature is varied so that the steam content in hydrogen sulfide remains constant (this provides constancy of the heat consumption per unit flow rate of the starting material). A pressure reduction by a factor of 3 or 5 would result in diminishing the separation column volume by 10 or 20%. In these calculations the throughput of the columns was assumed to be proportional to $\sqrt{P}$.

The temperature of hydrate formation can be reduced efficiently by introducing in the system a "third component", namely, a compound reducing water activity in solution, such as $AlCl_3$, $MgCl_2$, LiCl, KCNS, NaHS, and some organic compounds, e.g., monoethanolamine, hydrazine, and others. Figure 9 illustrates how the quadruple point and the curve of "solid crystal hydrate-aqueous solution of hydrogen sulfide" equilibrium shift upon introduction of one of the most efficient additives, KCNS (see Fig. 9, lines 4 and 5).

A correlation between the drop of the temperature of crystal hydrate formation ΔT_g and a decrease in the freezing point or increase in the boiling point of electrolyte solutions was found by Barret (19):

$$\Delta T_g = T_{O,g}^2 \left(\frac{m}{n} \frac{\Delta H_{ph}}{\Delta H_g} \frac{\Delta T_{ph}}{T_{O,ph}^2} + \frac{2.3R}{\Delta H_g} J h_0 \right), \tag{92}$$

where J is the ionic strength of electrolyte solution, h_0 is the proportionality coefficient calculated from the Barret data (19), ΔH_{ph} is the heat of water phase transition (evaporation or condensation), ΔH_g is the heat of decomposition of crystalline hydrate into water and gas (−66 kJ/mol), m and n are the numbers of water and gas molecules per molecule of crystalline hydrate.

The temperatures of hydrate formation were calculated from the ΔT values measured for freezing points of aqueous KCNS solutions. They are displayed in Fig. 9 by dashed lines, which shows a fairly good fit of calculations to measurements (solid lines).

The necessary condition for the practical use of additives decreasing the temperature of formation of crystalline hydrogen sulfide hydrate is to minimize the negative effect of these additives on the efficiency of isotope exchange in the columns. To explore the possibility of intensification of the GS process by changing the operation parameters of the process (reduction of pressure and temperature in the columns), special experiments were carried out in the set-up shown schematically in Fig. 11 (8) at subzero temperatures in the cold column.

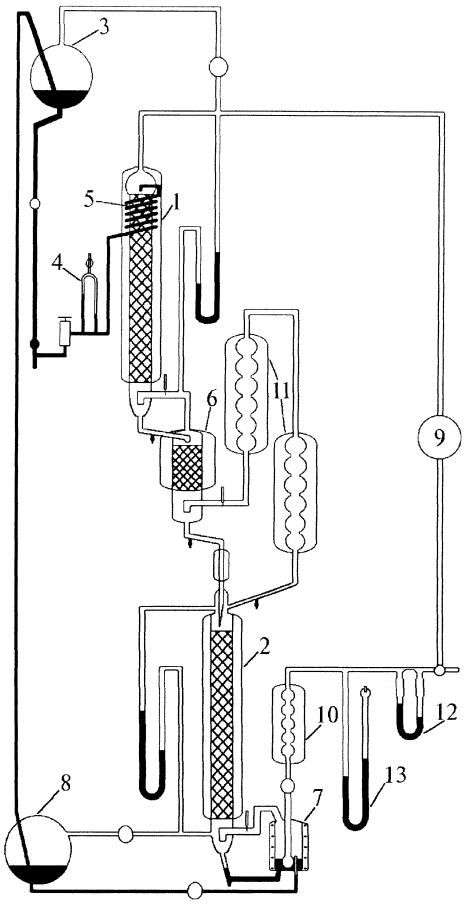

Figure 11. Scheme of laboratory-scale dual-temperature set-up (see text).

The major part of the set-up consists of two columns, one of them is cold (1) (the height of the packed section $h = 0.95$ m, diameter $d = 1.7$ cm) and the other is hot (2) ($h = 0.85$ m and $d = 2.4$ cm). The columns are filled with Levin's spiral-prismatic packing consisted of $2 \times 2 \times 0.2$-mm units. The feeding liquid saturated with hydrogen sulfide at room temperature is directed from tank (3) through flowmeter (4) and coil (5) mounted in the upper part of the column jacket to the cold column (1) where it is used as a refluxing liquid. By passing the column, the liquid is enriched with the heavier hydrogen isotope. Then the liquid is directed to heat exchanger (6) cooling the gas where it is heated and partially liberates dissolved hydrogen sulfide. After this, it feeds the hot column (2). By

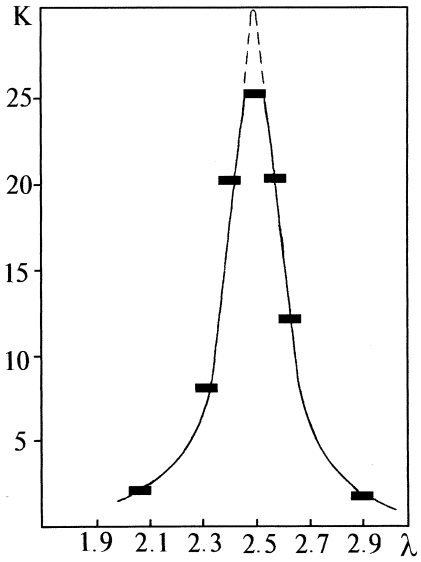

Figure 12. Dependence of separation degree (K) on ratio of flows (λ).

passing the hot column, the liquid is depleted with the heavier isotope and is poured in receiver (8) through saturator (7).

The gas flow produced by blower (9) is closed. Prior to entering the hot column, the gas goes through heater (10) and saturator (7) where it is heated to the desired temperature and humidified. After the hot column, the gas is directed to cooler (11) to separate the major part of steam and then to heat exchanger (6), from which the gas cooled to the necessary temperature is supplied to the cold column. The gas flow rate was measured with flowmeter (12) and the pressure in the cycle is recorded by a gauge (13). The temperature in the hot column was maintained at $T_2 = 333$ K, and to keep the temperature in the cold column at a constant level of $T_1 = 263$ K, a cooling loop was used.

Aqueous solution of KCNS (40 wt%) containing the additive enhancing isotope exchange was used in experiments. The initial deuterium concentration was 0.4 mol%. Water used in experiments on separation of H-T mixtures contained 10^{-5} Ci/liter of tritium. The steady-state separation degree attained in the set-up is presented in Fig. 12 as a function of the flow rate ratio λ. Note that at high separation degrees K the set-up did not operate in non-withdrawal mode as the liquid was periodically sampled for isotope analysis (from the enriching section of the set-up after heat exchanger (6)). This was taken into account in the treatment of experimental data. Thus, in experiments on separation of H-D mixtures, the fraction of sampled liquid was $\rho = P/L = 0.004$ and in separating H-T mixtures ρ

$= 0.0028$. Furthermore, the $K = f(\lambda)$ dependence presented in Fig. 12 was obtained at the ratio of heights of hot and cold columns, which differed from unity.

Since the upper section of heat exchanger (6) was operating as a separating column, the height of the cold part of set-up was markedly larger than one of the hot section and $\kappa_x = N_{1,x}/N_{2,x} = 1.23$. The separation degree used in calculations of NTU in separation columns was assumed to be $K = 19.6$ ($\theta = 0.36$) at a flow ratio $\lambda = 2.63$, in which the value differs from the optimal one.

As seen in Fig. 12, the K vs. λ dependence has a sharp maximum. As possible oscillations of λ in the set-up attain $\pm 1.5\%$, calculations of NTU by the maximum point give slightly different HTU values.

Calculations by Eq. (76) with accounting for the relative flow of withdrawal and mutual phase solubility (primarily of steam content in hydrogen sulfide, $h = 0.19$) gave the following results: $N_{1,x} = \chi_x$, $N_{2,x} = 46.7$ or $\mathrm{HTU}_{0x} = 2.25$ cm. The $K = f(\lambda)$ dependence denoted in Fig. 12 by a solid line was computed from the calculated NTU values. As seen, the results of calculations are in a good agreement with experimental data.

The results obtained in experiments on separation of H-T and H-D mixtures at the optimal flow ratio λ_0 are collected in Table 9.

As seen from the data of Table 9, a high separation efficiency is achieved for both H-D and H-T mixtures by using a laboratory-scale set-up with the cold column operating at low temperature and atmospheric pressure. A decrease of the temperature range $\Delta T = T_2 - T_1 = 70°$ did not reduce the α_1/α_2 ratio defining (at equality of other parameters) the attainable separation degree (Table 6). It is important to emphasize that introduction of the KCNS additive in the aqueous phase does not influence the efficiency of mass exchange. The HTU values in columns

Table 9. Results of Experiments on Separation of H-T and H-D Mixtures in Dual-temperature Set-up at λ_0, $\kappa_x = 1.23$, $T_1 = 263$ K, $T_2 = 333$ K, and $P = 0.105$ MPa (8)

Parameter		Separated Mixture	
		H-T	H-D
Separation factor	α_1	4.09	2.71
	α_2	2.35	1.87
Flow rate, mol/min	L	0.062	0.092
	G	0.23	0.23
Flow ratio	λ_0	3.69	2.5
Relative yield	θ	0.61	0.44
Separation degree	K	62.4	24.6
NTU $N_{1,x} = \kappa_x N_{2,x}$		45.2	44.1
HTU_{ox}, cm		2.32	2.38

of a dual temperature set-up, in this case, appear to be even a bit lower than those estimated from the results obtained by studying the kinetics of isotope exchange (8).

An alternative approach (besides the above-considered) to increase the α_1/α_2 ratio and, hence the separation efficiency, is based on an increase of temperature in the hot column and simultaneous by 3- to 5-fold increase of pressure in it (9).

A similar idea (i.e., to maintain different pressures in the cold and hot columns) underlies the patent (20), which suggests lowering T_1 to 293 K and to reduce the pressure to 7 atm with the aim of increasing the maximum extraction degree from 0.205 to 0.220. It is interesting to note that the cold column of the first commercial dual-temperature hydrogen sulfide plant built in the USSR in 1947 was working under almost identical conditions ($T_1 = 298$ K, $P_1 = 8.8$ atm) (21). However, due to unfavorable working parameters in the hot column, the efficiency of this plant was not high. Obviously, the effect must be most profound when both factors are used, i.e., the exchange columns operate at different pressures and the aqueous phase contains an additive precluding formation of crystalline hydrogen sulfide hydrates. The flow sheet of such a dual-temperature set-up is shown in Fig. 13.

Humid gas leaving the hot column at temperature T_2 is cooled due to adiabatic expansion in turbine (4) to pressure P_1 and is supplied to the cold column op-

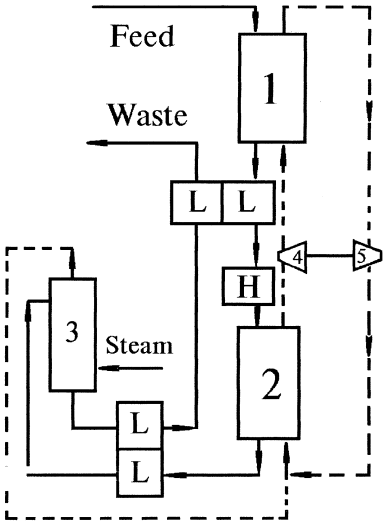

Figure 13. Scheme of dual-temperature set-up for separation of hydrogen isotopes in hydrogen sulfide-water system with cold and hot columns operating at differing values of pressure.

MARCEL DEKKER, INC.
270 Madison Avenue, New York, New York 10016

erating at temperature T_1. The external work produced by the turbine is used to compress the gas on its way from the cold column to the hot column in compressor (5). The use of turbine-compressor system allows for achieving a higher energy recuperation than in the units with heat exchangers, in which the phases are in direct contact. Indeed, the internal adiabatic efficiency of large gas turbines attains 0.85–0.92, and their mechanical efficiency reaches 0.95. Hence, the overall efficiency of a turbine can be estimated to be ~0.85. By accounting for a similar efficiency of the compressor accomplishing the reverse process the degree of energy recuperation appears to be 0.7. If the operation parameters were such that compression of the gas would increase its temperature from T_1 to T_2, the heat energy is to be consumed due to incomplete heat recuperation in the liquid-liquid heat exchangers.

Several publications describing two plants built in Kata and Manuguru, India (22,23) report some results obtained by the further development of the GS process. For example, unlike Canadian plants (the biggest in the world) where the coupling between separation cascade stages is accomplished through either gas or liquid flow, at plants in India the gas flow coupling with circulation of liquid flows at each stage is chosen as optimal. In doing so at the last third stage of the cascade a working option with circled gas flow is also provided to allow significant shortening of the steady-state achievement time after repeating start-ups and to exclude the deuterium transfer to the first two stages when the operation conditions are broken down. A possibility to use the GS process for separation of tritium containing hydrogen isotope mixture is also considered in the literature (8,24,25).

Finally, the economical efficiency of separation can be improved by using new process flow sheets providing enhancement of isotope exchange due to an increase of the driving force of the process and the possibility of operating with a closed cycle of the liquid phase of the optimal composition. Thus, the flow sheet with "source" column shown in Fig. 14 (8) seems to be of particular interest. The use of this set-up offers several advantages, such as lower sensitivity of the dual-temperature set-up to fluctuations of the feed flow, mitigation of the requirements imposed on purity of the feed, feasibility to utilize water-soluble additives (enhancing isotope exchange or inhibiting corrosion), and avoiding the stage of their removal from the waste flow. By increasing the feed flow in the "starting material" column, one can enhance performance of a dual-temperature set-up. The same effect may also be achieved by introducing an additional feed flow in the bottom part of the hot column (to a tray on which the deuterium concentration in water is identical to that in the starting material flow), provided the separation process is implemented according to the conventional dual-temperature flow sheet, i.e., without "source" column. As follows from the results of calculations reported by Babcock (26), an increase in the capacity of a hydrogen sulfide plant depending on the value of feed flow may attain 11%.

MARCEL DEKKER, INC.
270 Madison Avenue, New York, New York 10016

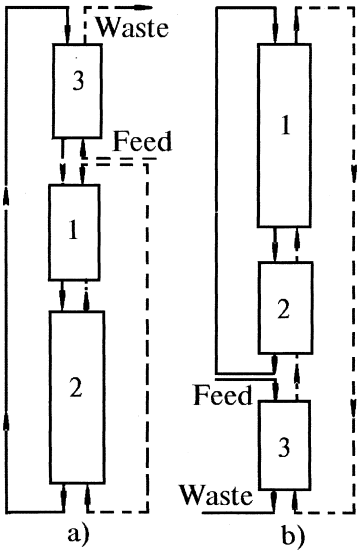

Figure 14. Schematic diagram of dual-temperature units with source column and liquid (a) or gas (b) feed. (1), cold column; (2), hot column; (3), source column.

The process scheme with source column (see Fig. 14a) is of particular interest when natural hydrogen sulfide is used as deuterium source. For example, in Russia, implementation of this process can be based on the use of the Astrakhan natural gas deposit with extremely high H_2S content. In this case, the costs related to production of heavy water are reduced as much as twice if the deuterium concentration in H_2S is the same as in natural water (27). The substantial cost reduction is determined by the following: at the optimal flow ratio λ the molar gas flow is approximately two times higher than that of the liquid phase, and the degree of deuterium extraction from the starting material, as it has been shown earlier, is determined only by the values of separation coefficients in the cold and hot columns.

CONCLUSION

In spite of nearly a half-century of experience in industrial utilization of the GS process, all modifications realized in practice were predominantly reduced to an increase in the size of columns and aggregates and to designing more efficient contact equipment (e.g., sieve trays) and heat recuperation facilities. At the same time, the flow sheet of the process and its operation parameters remained virtually invariable.

The analysis of new data on physico-chemical properties of the hydrogen sulfide-water system and on the kinetics of interfacial isotope exchange in contactors of different types allows one to formulate the following main routes to improve the efficiency of the GS process:

1. A tailored change of the operating parameters such as, pressure and temperature in the columns to increase the extraction degree and separation efficiency.
2. Enhancement (intensification) of isotope exchange by introducing activator additives and using packed mass-exchange columns (contactors).
3. Development of new separation flow sheets to intensify isotope exchange due to an increase of the process driving force, which permits operation with a closed cycle of the liquid phase of the optimal composition.

Realization of these modifications will not only make the GS process more efficient in production of heavy water but will also extend the area of its application primarily to decontamination from tritium of wastes of nuclear power plants.

LIST OF SYMBOLS

A	light isotope.
B	heavy isotope.
D_{H2S} and D_{H2O}	coefficients of molecular diffusion of hydrogen sulfide dissolved in water and of self-diffusion of water, respectively.
G_i and L_i	molar flows of gas and liquid phases in column i ($i = 1, 2$).
G_{sp} and L_{sp}	specific molar flows of gas and liquid phases in column.
$G_{y,i}$ and $L_{x,i}$	gas flow of substance Y and vapor flow of substance X.
G_i^*	gas-vapor flow.
H_i	height of column.
K_{ox} and K_{oy}	mass-transfer coefficients in liquid and gas phases, respectively.
K_p and K_w	separation degrees in concentration and depletion sections, respectively.
$L_{x,i}$ and $L_{y,i}$	flow of liquid X and dissolved gas Y.
L_i^*	flow of liquid with dissolved gas.
$N_{x,i}$ and $N_{y,i}$	number of transfer units (NTU) for liquid and gas phases.
S_i	cross-section.
Z_i	coordinate along column height.
a_i	interphase surface per unit of column volume.
d_e	equivalent size of channels.
h_i	content of evaporated liquid X in gas Y [mol X/mol Y].

MARCEL DEKKER, INC.
270 Madison Avenue, New York, New York 10016

h_{ox} and h_{oy}	height of transfer unit (HTU) for liquid and gas phases.
h_x and h_y	components of HTU determined by mass-exchange in liquid and gas phases.
n_i	number of theoretical plates (NTP).
k_F^* and k_R^*	constants for direct and reverse reactions of pseudo-first order.
s_i	solubility of gas *Y* in liquid *X* [mol *Y*/mol *X*].
x_i and y_i	atomic fraction of deuterium in water and hydrogen sulfide, respectively.
x_g	isotope concentration in vapor of substance *X*.
y_l	isotope concentration in substance *Y* dissolved in liquid *X*.
Γ_m	maximal extraction degree.
α_i, α_{gl}	separation factor for reaction of isotope exchange proceeding between liquid phase *X* and gas phase *Y*.
α_g	separation factor for reaction of isotope exchange in gas phase.
α_x	separation factor at liquid-vapor phase equilibrium of substance *X*.
β_c	chemical component of mass-transfer coefficient.
λ_i	flow ratio ($\lambda_i = G_i/L_i$).
λ_o	optimal flow ratio.
θ	relative withdrawal.
τ	time.

REFERENCES

1. Andreev, B.M.; Zelvensky, J.D.; Katalnikov, S.G. *Physico-Chemical Methods for Separation of Stable Isotopes*; Energoatomizdat: Moscow, 1982. (in Russian)
2. Bron, I.; C.F. Chang; Wolfsberg, M. Z. Naturforsch. **1973**, *29A*, 129.
3. Van Hook, W. J. Phys. Chem. **1968**, *72*, 1234.
4. Bigeleisen, J. *Isotope Separation*, In Proc. Int. Symp., Amsterdam, 1957; Aoc NierNorth Holland Publ. Co.: Amsterdam, 1958; 121.
5. Rozen, A.M. *Theory of Isotope Separation in Columns;* Atomizdat: Moscow, 1960. (in Russian)
6. Andreev, B.M.; Zelvensky, J.D.; Uborsky, V.V. At. Energ. (Atomic Energy) **1978**, *44*, 240. (in Russian)
7. Andreev, B.M.; Petrov, V.V.; Uborsky, V.V. Dokl. Akad. Nauk SSSR, **1980**, *235*, 1431. (in Russian)
8. Andreev, B.M.; Rakov, A.; Rozenkevich, B.M.; Sakharovsky, Y.A. Radiokhimia (Radiochemistry) **1997,** *20*(2), 97. (in Russian)

9. Andreev, B.M.; Zelvensky, J.D.; Katalnikov, S.G. *Heavy Hydrogen Isotopes in Nuclear Technology*; Energoatomizdat: Moscow, 1987. (in Russian)
10. Andreev, B.M.; Magomedbekov, E.P.; Rozenkevich, B.M.; Sakharovsky, Y.A. *Heterogeneous Reactions of Tritium Isotope Exchange*, Editorial URSS: Moscow, 1999. (in Russian)
11. Bier, K. Chem. Ing. Techn., **1956**, *29*, 625.
12. Andreev, B.M.; Uborsky, V.V. Teor. Osnovy Khim. Techn. (Theoretical Fundamentals of Chemical Technology) **1981**, *15*, 664. (in Russian)
13. Andreev, B.M. Khim. Prom. (Chemical Industry) **1962**, *N8*, 35. (in Russian)
14. Filippov, G.G.; Sakodinsky, K.I.; Zelvensky, J.D. Khim. Prom. **1965**, *N1*, 10. (in Russian)
15. Andreev, B.M.; Katalnikov, S.G. Khim. Prom. **1965**, *N4*, 268. (in Russian)
16. Burgess, M.P.; German, R.P. AICHE J. **1969**, *15*, 272.
17. Burgess; M.P. AICHE J. **1971**, *17*, 529.
18. Andreev, B.M.; Zelvensky, J.D.; Maslov, D.N. Gas. Prom. (Gas Industry) **1979***, N2*, 61. (in Russian)
19. Barret, V.L. *Gas Absorption on a Sieve Plate*, Ph.D. Thesis, Cambridge, UK, 1966.
20. Babcock, D.F. Dual Pressure-Dual Temperature Isotope Exchange Process. US Patent 3,792,156, 1974.
21. Rozen, A.M. At. Energ. **1995**, *78*(3), 217. (in Russian)
22. Sonde, R.R.; Kamath, H.S.; Bhargava, R.K.; Sharma, S. In *Proc. National Symposium on Heavy Water Technology*, Bombay, India, April 3–5, 1989; PD-2.
23. Agarwal, A.K.; Verma, A.N. In *Proc. National Symposium on Heavy Water Technology*, Bombay, India, April 3–5, 1989; PD-12.
24. Croitoru, C.; Pavelescu, M. Rom. Rep. Phys. **1996**, *48*(9–10), 819.
25. Andreev, B.M.; Zelvensky, J.D. Khim. Prom. **1999**, *N4*, 208. (in Russian)
26. Babcock, D.F. Isotope Enrichment, Especially of Deuterium, US Patent 3,549,323, 1969.
27. Andreev, B.M.; Magomedbekov, E.P.; Park, Y.S.; Rozenkevich, B.M.; Sakharovsky, Y.A.; Selivanenko, I.L.; Uborsky, V.V. At. Energ. **1999**, *86*(3), 198.

MARCEL DEKKER, INC.
270 Madison Avenue, New York, New York 10016

Request Permission or Order Reprints Instantly!